Review

Artificial Intelligence in Symptomatic Carotid Plaque Detection: A Narrative Review

Giuseppe Miceli [1,2,*] **, Giuliana Rizzo** [1,2] **, Maria Grazia Basso** [1,2] **, Elena Cocciola** [1,2] **, Andrea Roberta Pennacchio** [1,2] **, Chiara Pintus** [1,2] **and Antonino Tuttolomondo** [1,2]

[1] Department of Health Promotion, Mother and Child Care, Internal Medicine and Medical Specialties (ProMISE), Università degli Studi di Palermo, Piazza delle Cliniche 2, Via del Vespro 129, 90127 Palermo, Italy
[2] Internal Medicine and Stroke Care Ward, University Hospital, Policlinico "P. Giaccone", 90100 Palermo, Italy
[*] Correspondence: miceli.gpp@gmail.com; Tel.: +39-0916552115; Fax:+39-0916552142

Abstract: Identifying atherosclerotic disease is the mainstay for the correct diagnosis of the large artery atherosclerosis ischemic stroke subtype and for choosing the right therapeutic strategy in acute ischemic stroke. Classification into symptomatic and asymptomatic plaque and estimation of the cardiovascular risk are essential to select patients eligible for pharmacological and/or surgical therapy in order to prevent future cerebral ischemic events. The difficulties in a "vulnerability" definition and the methodical issues concerning its detectability and quantification are still subjects of debate. Non-invasive imaging studies commonly used to detect arterial plaque are computed tomographic angiography, magnetic resonance imaging, and ultrasound. Characterization of a carotid plaque type using the abovementioned imaging modalities represents the basis for carotid atherosclerosis management. Classification into symptomatic and asymptomatic plaque and estimation of the cardiovascular risk are essential to select patients eligible for pharmacological and/or surgical therapy in order to prevent future cerebral ischemic events. In this setting, artificial intelligence (AI) can offer suggestive solutions for tissue characterization and classification concerning carotid artery plaque imaging by analyzing complex data and using automated algorithms to obtain a final output. The aim of this review is to provide overall knowledge about the role of AI models applied to non-invasive imaging studies for the detection of symptomatic and vulnerable carotid plaques.

Keywords: artificial intelligence; ischemic stroke; machine learning; deep learning; toast classification

1. Introduction

Stroke is the fifth cause of death and the first cause of disability in the United States, with an increase in prevalence due to demographic changes. Eighty-seven percent of strokes in the United States are ischemic.

According to the Trial of Org 10172 in Acute Stroke Treatment (TOAST) classification, the large artery atherosclerosis (LAAS) subtype accounts for the etiology of ischemic stroke in 30% of cases, with mortality higher than other ischemic stroke subtypes [1–3]. The presence of large-dimension or vulnerable atherosclerotic plaques causing stenosis of more than 50% in one of the carotids, vertebral, or cortical circle arteries may result in the reduction of blood flow to the cerebral tissue [4,5].

Thus, atherosclerosis is considered a complex condition which can trigger ischemic stroke [6]. Identifying atherosclerotic disease is the mainstay for the correct diagnosis of LAAS and choosing the right therapeutic strategy in acute ischemic stroke. The timing of diagnosis is crucial for time-related treatments, which then allow an improvement in clinical outcomes and a reduction in disability [7–14].

Risk factors for atherosclerosis include hypertension, hyperlipidemia, diabetes, obesity, smoking, and a sedentary lifestyle [15,16].

Non-invasive imaging studies commonly used to detect arterial plaque are computed tomographic angiography (CTA), magnetic resonance imaging (MRI), and ultrasound (US).

Characterization of carotid plaque type with the abovementioned imaging modalities represents the basis for carotid atherosclerosis management. Classification into symptomatic and asymptomatic plaque and estimation of the cardiovascular risk are essential to select patients eligible for pharmacological and/or surgical therapy in order to prevent future cerebral ischemic events.

In this setting, artificial intelligence (AI) can offer suggestive solutions for tissue characterization and classification regarding carotid artery plaque imaging by analyzing complex data and using automated algorithms to obtain a final output [17]. This review analyzed the application of AI for the diagnosis of symptomatic carotid plaque, articulating the discussion per imaging modality, starting from research on ultrasound to MRI (see Figure 1). Finally, future perspectives on AI applications in carotid plaque diagnosis are briefly discussed in a separate section.
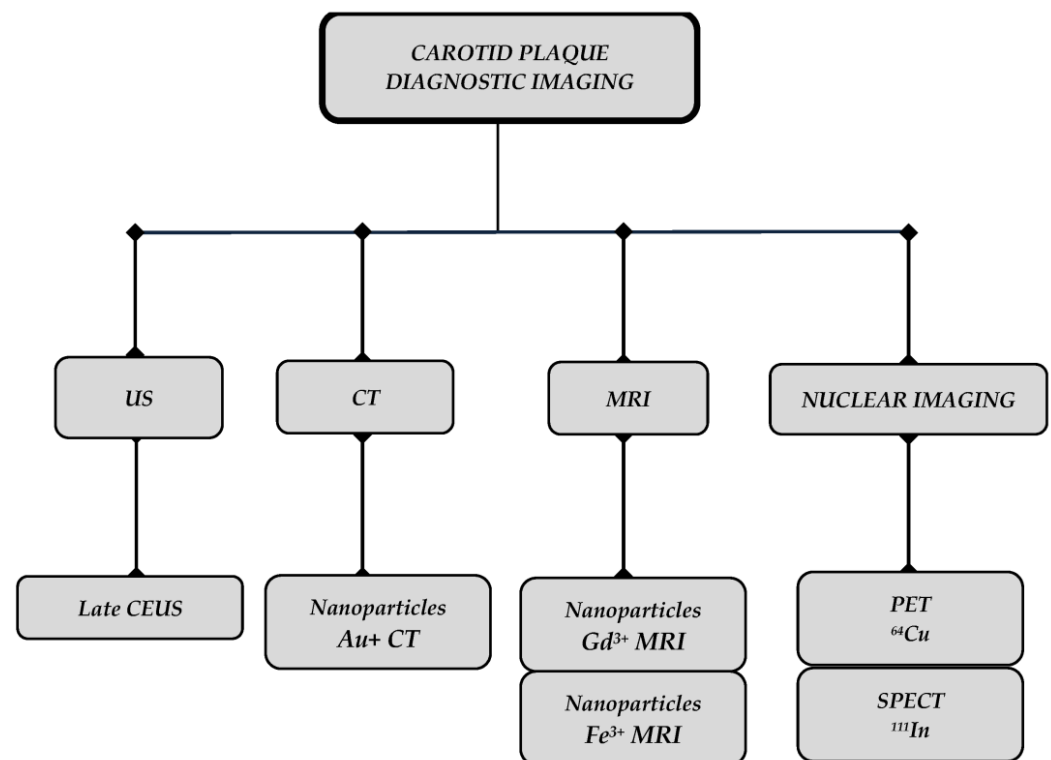

Figure 1. A step-wise approach to atherosclerotic plaque identification and characterization. Diagnosis and characterization of atherosclerotic plaque requires the employment of diagnostic image techniques. Among these, a first-line approach is represented by Doppler ultrasound, following CT and MRI scans. Recently, other techniques have been proposed to improve diagnosis and, mainly, identification of plaque features which could be predictive of its vulnerability and hence patient outcome. These techniques investigate plaque's molecular composition and are focused on detecting its inflammatory elements and targeting antigen overexpression, thus amplifying diagnostic potential at our disposal. US, ultrasonography; CT, computed tomography; MRI, magnetic resonance imaging; PET, positron emission tomography; SPECT, single photon emission computed tomography; CEUS.

The aim of this review is to provide the most effective state-of-the-art AI models used to improve the detection and diagnosis of symptomatic carotid plaque.

2. Overview of Artificial Intelligence

AI refers to the branch of computer science that studies the simulation of human intelligence in machines to obtain results, such as the extraction of information content

and production of new knowledge from datasets of great size and complexity. It involves the development of algorithms that can perform tasks that would typically require human intelligence, such as decision-making, problem-solving, and learning. AI can be divided into several subfields, including machine learning (ML), deep learning (DL), and computer vision. Some recent successes in the field of AI belong to the field of machine learning (ML), the sector that focuses on the development of algorithms that can learn from data and make predictions or decisions based on that data. It involves training models on large datasets to identify patterns and make predictions or decisions about new data. ML algorithms can be supervised, unsupervised, or semi-supervised, depending on the type of data used for training [18–20]. Supervised machine learning is a technique that involves training an algorithm on labeled data, where each data point is associated with a target output. The algorithm learns to map input features to the correct target output by minimizing the difference between its predicted output and the true output. The main algorithms used in supervised learning are linear regression models, tree-based and nearest-neighbor algorithms, support vector machines (SVMs), and deep neural networks. Unsupervised machine learning, on the other hand, involves training an algorithm on unlabeled data where there is no predefined target output. The algorithm learns to identify patterns or structures in the data by clustering similar data points or reducing the dimensionality of the data. Unsupervised learning can be used for tasks such as anomaly detection, customer segmentation, and recommendation systems. Finally, learning with reinforcement develops an artificial agent that must achieve a goal and, based on the contribution of the environment and the outcome of its actions, learns the best strategy to achieve the same goal. In the "traditional" approaches of machine learning, variables are derived either directly from clinical data or through measurements made by the operators. Thanks to the use of new artificial neural network architectures (ANNs), it is now possible to simplify the data extrapolation step. In this process, input variables are transformed, combined, and simultaneously classified. DL is a branch of ML that has evolved to analyze data, taking advantage of the layered structure of ANNs designed for specific tasks and to solve complex problems [21]. The main architectures used to analyze data provided in DL are convolutional neural networks (CNNs), recurrent neural networks (RNNs), and their subtypes, gated recurrent units (GRUs) and long-term memory networks [22]. The architecture of an ANN is formed by a series of inputs, hidden and output neurons, arranged on various levels, interconnected both within a layer and between layers. If the machine reaches the goal, the connection between those neurons is enhanced, otherwise, it weakens. Through this mechanism, the algorithm is automatically refined until a high degree of accuracy is reached. CNNs are a type of deep learning model that is particularly well-suited for image recognition tasks. CNNs are designed to process images by applying convolutional filters to the image pixels, which allows them to identify spatial patterns and features in the image. The layers composing the CNN framework can be divided into four types: a convolutional layer acting as a filter; a pooling layer sampling characteristics; a fully connected layer serving classification labels; and a non-linearity layer with an activation function. These types of models used in DL require a very large amount of data and can store an extremely large number of relationships between variables. The model is able to perform "intelligent" actions, but the user is not able to understand the operation of the system itself. Due to this, the behavior of an AI system is seen as a "black box". Activation maps and heatmaps are methods that attempt to address the problem of the "black box" but still require human intervention [23,24].

3. Symptomatic and Asymptomatic Carotid Plaques: From Pathophysiology to Diagnostic Issues

Atherosclerosis has classically been defined as an immune–inflammatory disease based on the implication of the innate and adaptive immune system and inflammatory cytokines in causing vascular damage, which constitutes the foundation of atherogenesis and plaque formation and perpetuation.

Several cytokines have been recognized as critical triggers in the development of atherogenesis. Among these, IL-1 has an essential role in the beginning and progression of atherosclerotic plaque, also representing a marker of risk for atherosclerotic disease severity [25]. In this concern, anti-IL-1 drugs have been proposed as a therapeutic strategy for the treatment of atherosclerotic disease [26,27]. Other cytokines taking part in the atherogenic processes are IL-18, TNF, and INF-y [28,29].

With regard to the role of the innate immune system, monocytes are the main cells involved in atherosclerosis development. After migration from peripheral blood to the intima and media layers of the vascular wall, monocytes turn into resident macrophages which are able to secrete proinflammatory cytokines (such as IL-1) responsible for the perpetuation of the local inflammation. The role of monocytes is supported by several studies that have found a correlation between peripheral monocytosis and the risk of atherosclerosis as well as the finding of increased levels of these cells within atherosclerotic plaques [30]. Dendritic cells and neutrophils are also involved in the pathogenesis of atherosclerotic disease, inducing vascular damage through the accumulation of lipid products into the "foam cells" and the production of reactive oxygen products and neutrophil extracellular traps recruiting monocytes from peripheral blood [31–33].

The adaptive immune system participates in the formation of plaque with different roles on the basis of the different cell subtypes. In fact, T-helper 1 cells have a proinflammatory profile promoting atherogenesis [34], while the contribution of T-helper 2 and T-helper 7 is still not well understood [35].

Atherosclerotic plaques show a high accumulation of CD8-T cells, suggesting the possible role of these cells in atherosclerotic disease due to the secretion of proinflammatory cytokines [36]. The role of B cells is still unclear, even though a proatherogenic role has been suggested, given their ability to suppress T cells in lymphoid organs [37].

Moreover, other elements extraneous to the plaque itself are involved in its evolution. Atherosclerotic lesion disruption, in fact, causes the exposition of thrombogenic material to the bloodstream, and this represents the *zero point* of plaque's progression. In particular, the tissue factor (TF) is considered the primary trigger of the activation of the coagulation cascade in atherosclerotic plaque progression, as also demonstrated by the finding of elevated TF levels in patients with PAD, mainly in early atherosclerotic lesions, suggesting a strong early procoagulant milieu [38,39].

As confirmation of the interaction between inflammation and coagulation in the pathogenesis of atherosclerosis, high expression of thrombin, factor X, TF (tissue factor), and FXII in atherosclerotic plaques and intima–media thickening has been reported in several studies, suggesting the critical role of coagulation not only in the progression but also in the early development of atherogenesis [40,41].

Furthermore, clotting factors (in particular TF, factor Xa, and thrombin) induce inflammation through the activation of PAR (protease-activated receptor) pathways, leading to the proliferation of smooth muscle cells, the adhesion of leukocytes on the vessel wall, the activation of proinflammatory signals (NfKb pathway and production of cyclo-oxygenase), and platelet aggregation on the vascular surface [42–44].

The progression of the atherosclerotic plaques leading to volume increase and vulnerability depends on the cell subtypes infiltrating the arterial wall [45]. Monocytes and macrophages in the atherosclerotic plaques are responsible for core necrosis and local thrombosis due to the production of matrix-degrading proteases and the release of tissue factors and lipids [46]. The adaptive immune system is also involved in the development of atherosclerosis, with a proatherogenic role of T-helper and B cells as opposed to the anti-atherogenic role of regulatory T cells [35,47].

Given the role of immune cells in the progression of atherosclerosis, new models based on AI have been proposed in order to predict the risk of acute ischemic stroke on the basis of the recognition of the cellular composition of the atherosclerotic lesion using histopathological samples obtained from patients who underwent endarterectomy. In this concern, Wang et al. [48] proposed a machine learning method (called CIBERSORT) com-

bined with LASSO regression for differentiating cellular infiltration in stable and unstable plaques. They found a significantly higher expression of M0, M1, and M2 macrophages in the unstable lesions than in the stable lesions where T cells were predominant.

Atherosclerotic plaques are the main cause of acute cardiovascular and cerebrovascular events [49]. They have different characteristics reflecting the affected district and composition that influence plaque's susceptibility to rupture or erosion. Apart from coronary lesions, peripheral artery disease plaques present a prevalent composition of collagen, smooth cells, and calcifications, which provide the plaque with higher stability [49,50].

The modified American Heart Association (AHA) classification [49] categorizes, in a practical way, atherosclerotic plaques with the aim of highlighting their image appearance and recognizes (i) adaptive intimal thickening (AIT), (ii) pathological intimal thickening (PIT), (iii) fibroatheroma (FA), and (iv) fibrocalcific plaque (FC).

Although for many years, the size of the plaque and the degree of luminal vessel narrowing have been considered pivotal in ischemic cardiovascular disease pathogenesis [51], nowadays, the importance of plaque qualitative properties, together with its thickness and dimensions, is recognized.

Several determinants can be used to describe plaque characteristics: (i) symptomatic or asymptomatic; (ii) the degree of the stenosis; and (iii) vulnerability.

According to the European Stroke Organisation guideline on endarterectomy and stenting for carotid artery stenosis [52], carotid stenosis is defined as *symptomatic* if it has caused ischemic cerebrovascular events in the ipsilateral eye (transient monocular blindness or retinal infarction) or cerebral hemisphere (transient ischemic attack (TIA) or stroke) in the preceding six months and *asymptomatic* if it is not associated with any ocular or cerebral ischemic events in the ipsilateral carotid territory within the preceding six months. The term "symptomatic" is then related to the presence of clinically overt manifestations of vessel alterations.

Stenosis and Vulnerability

Carotid artery stenosis (CAS) is usually associated with plaque progression and accounts for 10–20% of ischemic strokes due to atherothrombotic diseases. Moreover, the risk of the first ischemic stroke, as well as the risk of its recurrence, is proportional to the degree of stenosis [53,54].

Several non-invasive imaging techniques are used to stratify the risk of atherosclerotic plaques and assess the narrowing of the lumen diameter: magnetic resonance imaging (MRI), computed tomography (CT), positron emission tomography (PET), single photon emission computed tomography (SPECT), and ultrasound imaging (US) [55].

These techniques can help the physician stratify the stenosis into three categories: (i) mild (<50%), (ii) moderate (50–69%), and (iii) severe (70–99%).

However, although the degree of stenosis has historically been considered a key element in atherosclerotic cardiovascular disease risk determination and establishing the need for surgical treatment in both symptomatic and asymptomatic carotid stenosis, it is not sufficient per se for stratifying the risk of a future stroke, as observed in both the NASCET [56] and ECST [57] trials. In fact, authors observed that more than 40% of strokes during follow-up occurred in patients with CAS < 50%, and more than 80% of patients with CAS > 50% did not suffer a stroke event during the five years of follow-up.

Hyafil et al. [58] reported that more than 20% of carotid arteries with mild stenosis (<50% stenosis) and about 8–9% of carotid arteries with normal lumen size are found to have features of vulnerability.

Additionally, the American Society of Neuroradiology and the European Society of Cardiology (ESC) propose the risk of carotid-vulnerable plaque rupture should also be attributed to plaque compositions rather than only to plaque size [59,60].

However, the difficulties in the "vulnerability" definition and the methodical issues regarding its detectability and quantification are still subjects of debate.

The term *vulnerability* is used to refer to plaques that are susceptible to complications and can, thus, be prone to the occurrence of thrombotic phenomena or rapid progression [61].

Additionally, it has been proposed to indirectly identify vulnerability through the evidence of some elements, such as intraplaque hemorrhages, lipid-reach necrotic cores, and microembolization in cerebral arteries, resorting to second-level diagnostic tests, such as MRI sequences using standardized protocols and transcranial Doppler [62–65].

MRI has the value of providing detailed morphological information about the artery wall, luminal area, and plaque composition, although it has the disadvantage of having a long scan time and is not suitable for every patient (such as patients with metal devices).

One of the best-validated techniques to identify plaque with a risk of embolization is transcranial Doppler. A prospective single-center study of 319 patients showed that the absence of transcranial microemboli detection in asymptomatic stenosis identifies low-risk patients that will not benefit from endarterectomy or stenting [66]. Another prospective multi-center international study conducted on 467 patients demonstrated that the detection of asymptomatic embolization on transcranial Doppler can be used to identify high-risk patients with asymptomatic carotid stenosis [67].

Routine computed tomography angiography (CTA) can provide a qualitative, semi-quantitative, and quantitative evaluation of the vulnerability of atherosclerotic plaque and has been used for the characterization of carotid artery tissue.

On the other hand, daily routine quantification of vascular diseases in carotid vessels is currently restricted to manually measured criteria, such as those described by NASCET and ECTS [68]; CTA showed very good results in detecting ulcerations [69,70], identifying rupture of the fibrous cap [71], the evaluation of inflammation, and the extent of neovascularization, with the degree of postcontrast plaque enhancement [72].

Indeed, the interpretation of CTA findings regarding the degree of carotid stenosis and its characteristics has not been standardized yet, and the technique is subject to many limitations, including the use of radiation, contrast medium, and motion artifacts [73].

An easily performable and available technique is ultrasound (US) which is also time-efficient and has better patient tolerability [74].

In recent years, several vascular ultrasound methods have been investigated to characterize vulnerable plaque, such as elastography and contrast-enhanced ultrasound (CEUS).

Elastography assesses carotid plaques' mechanical properties by measuring their deformation (called strain), in particular considering the measure of plaque deployment caused by blood pressure oscillations. In fact, unstable plaques are characterized by displacement patterns in relation to their composition, so vulnerable plaques (in which we can see elements such as intraplaque hemorrhage) are characterized by considerable deformation [75–77].

CEUS of the carotid artery is applied through the injection of echogenic gas-filled microbubbles into the circulation using available agents. The study of the movement of microbubbles is performed in the lumen (bloodstream), the vasa vasorum, and the intraplaque microvessels, whose presence derives from the processes of angiogenesis taking place inside the vulnerable plaque in response to hypoxia secondary to plaque thickness and high metabolic demand [78,79].

The application of AI in the study of atherosclerotic disease aims to build an integrative model by integrating clinical, laboratory, and instrumental features for patient cardio- and cerebrovascular risk stratification (Figure 2).
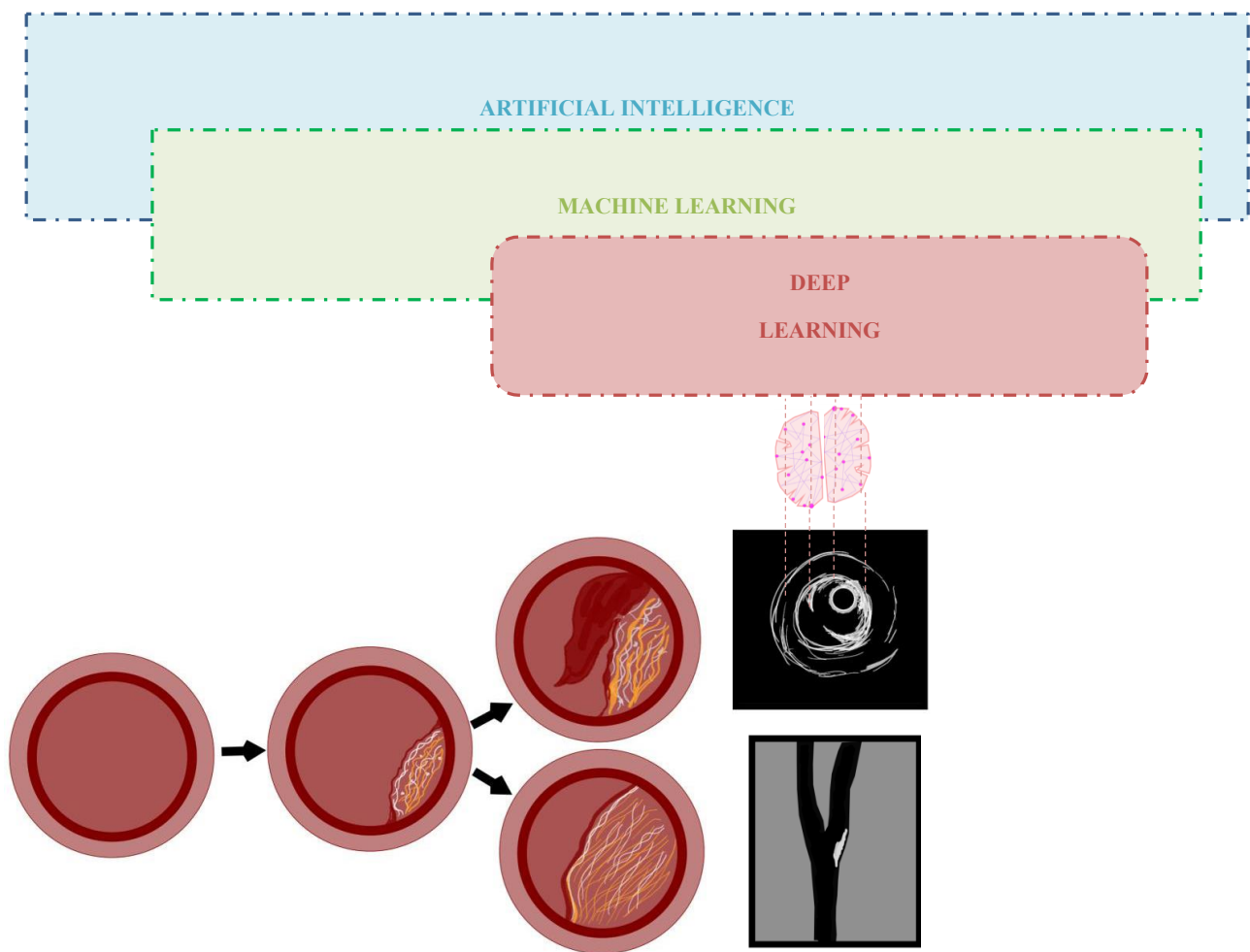
Figure 2. Artificial intelligence and imaging techniques for symptomatic plaque detection. Atherosclerotic plaque's evolution is expressed by two major terms "stenosis" and "vulnerability". These two possible scenarios can be detected thanks to several diagnostic imaging tools. Images can be acquired and elaborated by deep learning patterns, which could make image interpretation faster and more accurate, overcoming some human bias.

4. Artificial Intelligence in Ultrasound in Symptomatic Carotid Plaque

As proposed in the SCOT-HEART and PROMISE II trials [80,81], the vulnerability of plaque more than its size is responsible for acute vascular events: the rupture of the plaque causes distal embolization or intralesional thrombosis, resulting in the reduction of blood flow [82,83].

The vulnerability of plaque depends on morphological and hemodynamic characteristics: hemodynamic factors, such as blood flow volume and velocity, wall shear stress, energy loss, and pressure gradient acting on the plaque surface are the main determinants of the progression of atherosclerotic lesions [84]. Due to the reduction in the vascular lumen and the increased blood flow velocity, high wall shear stress is the primary burden for endothelial cell damage leading to plaque rupture. Ultrasound study is the most widely used technology for the non-invasive examination of carotid disease, allowing the assessment of the morphologic plaque characteristics and the evaluation of the alteration of the hemodynamic factors through the modification of the wave velocity profile on the power Doppler.

Carotid Doppler ultrasound may stratify the carotid plaque vulnerability based on the echogenicity and surface profile of lesions. However, this technique depends on the operator's ability and experience and cannot identify the internal compounds, reducing

the accuracy in establishing the vulnerability. Ultrasound instability characteristics are hypoechogenicity, an irregular surface, an incomplete fibrous cap, or a plaque blood flow signal suggestive of ulceration [85].

Conventionally, ML and DL strategies may be used to evaluate atherosclerotic carotid disease. Artificial intelligence consists of extracting, analyzing, and interpreting imaging features by developing complex algorithms producing predictive results [86,87]. This technology is termed "radiomics".

The application of AI in carotid disease provides automated segmentation methods to ameliorate the work of physicians. Segmentation methods can be based on traditional image processing, requiring more accuracy and expert evaluation. Deep learning-based segmentation methods have been designed to increase diagnostic accuracy in recent decades. However, imaging omics are primarily created from CT and MRI scans, while only a few studies have evaluated the application of AI using vascular ultrasound assessment.

4.1. AI Based on Ultrasound Images for Automatic Carotid Segmentation

Promising results have been reached in applying a CNN in a U-shaped structure (U-Net) for automatic segmentation. This model uses contracting or encoding layers followed by up-sampling or decoding layers and skip connections to increase the resolution of the output. U-Net has been used in one study by Zhou et al. to identify carotid stenosis in more than 60% using 3D ultrasound datasets, obtaining a high accuracy (Dice coefficient 0.9). However, the study was not accurate enough, considering the fewer subjects selected (13) [88].

Dilated convolution networks represent another CNN architecture with the advantage of no need for down- and up-sampling. A combination of U-Net and dilated convolution networks offers the best carotid segmentation method [89,90]. The application of dilated U-Net [91] has shown to be better in under-performing conditions and the case of complex plaques with a Dice coefficient of 0.88, compared to the value of 0.77 for U-Net alone, while no differences were reported in the better-performing situations. The low value of the Dice coefficient compared with the study reported by Zhou et al. could derive from the different methodologies used to detect US images. In fact, Zhou et al. used a 3D model that is more accurate than the 2D datasets generated from research data in the latter study. Moreover, the model could perform carotid segmentation in healthy people without arterial plaques, as confirmed by other studies [92–94].

Despite the better performance of dilated U-Net, this model presents some limitations, such as the need to resort to a sonographer input via a bounding box on the plaque to achieve an acceptable segmentation performance (semi-automated segmentation) and the reduction of the accuracy in the case of the presence of acoustic shadowing. Therefore, new CNN models have been proposed to pose the bounding box correctly before the segmentation to reduce errors [95,96].

These data were confirmed in more recent studies using layered deep learning U-Net architecture for carotid wall segmentation using images from US studies. Jain et al. conducted one study on two different demographic groups of patients (a Japanese cohort and a Hong Kong cohort) with atherosclerotic carotid disease. The study showed good accuracy, dice similarity, and correlation coefficient (>90, >75, and >0.80%, respectively) in detecting and classifying carotid plaques. However, including the noisy Hong Kong database in the system and the high-intensity zone of the media region of the plaques did not allow for performing the best partial volume in the region of interest [97].

4.2. Application of AI for Vulnerability Plaque Assessment

In another study, the application of deep learning models (in particular CNN-based models and U-Net) using 2D ultrasound imaging was a suitable methodology for the automated classification of plaques into vulnerable and stable lesions [15].

Furthermore, Zhang et al. [75] conducted a study to propose a new model based on ultrasound images in combination with a LASSO algorithm to assess the stability of

atherosclerotic plaques using ultrasound images. The study population comprised 150 patients with acute ischemic stroke or transient ischemic attack in whom carotid plaques were detected using ultrasound and high-resolution magnetic resonance examination. The model was created based on four conventional ultrasound carotid features: surface morphology, expression of the fibrotic cap, echogenicity, and ulceration, identifying 83 vulnerable and stable plaques, with an accuracy, sensitivity, and specificity of 79.05, 85.94, and 68.29%, respectively. In addition, the logistic regression model was used to create a conventional ultrasound–texture feature combined model for the automated identification of stable and unstable plaques: the combined model had a high accuracy, sensitivity, and specificity (84.76, 77.94, and 97.30%) and was based on eight statistically significant features extracted from the ultrasound images of carotid plaques. Unfortunately, the study presents some limitations, such as selection bias derived from the bidirectional cohort study; bias derived from the manual measurement of the plaques; the relatively small size sample; and the lack of histopathological confirmation [98].

Moreover, an optimized system (DCNN11A5) [99] using the mean of the feature strength (MFS) has been proposed for computed plaque characterization, distinguishing symptomatic and asymptomatic plaque based on echogenic characteristics and surface regularity. This model was proposed in a study by Skandha et al. conducted on a population cohort of 346 patients (196 patients with symptomatic plaque and 150 with asymptomatic plaque) whose images from internal carotid arteries were obtained by an echocolor Doppler study. 36 Diffusion convolutional neural network (DCNN) combinations were analyzed to find the best DCNN model under augmentation, showing that 3D optimization (called DCNN11A5) resulted in the best-performing model. This model was able to distinguish symptomatic and asymptomatic plaques based on the MFS, finding higher values in the first than the latter condition with an accuracy of 95.66% (AUC 0.956, $p < 0.0001$). The DCNN11A5 model appeared to be more accurate than other ML methods, providing an improvement of 7.01% ($p < 0.0001$) in the identification of plaque vulnerability. In the same study, bispectrum strength computation was used by applying the Radon transform to all the US images collected for the calculation of the B value in the two groups of patients; in particular, B values in symptomatic plaques were 5.4% higher than in asymptomatic plaques.

In conclusion, the study proposed two new automated models which are able to provide an additional useful tool to support the need for invasive therapeutic strategies (endarterectomy or stenting) on the basis of plaque characteristics linked to vulnerability risk. The small size of the cohort and the limited availability of the supercomputer during the study affected the strength of the results of the study.

Given the role of hemodynamic factors on the stability and the progression of plaques, a combined computational 3D geometry technology based on carotid artery ultrasound data collected in hospital practice was created to identify complex flow features in the case of critical carotid stenosis [99]. In one study performed on a population cohort of 346 patients (196 patients with symptomatic plaque and 150 with asymptomatic plaque) whose images from internal carotid were obtained by Doppler study, the MFS values in symptomatic plaque were higher than in asymptomatic plaques. In the same study, the application of bispectrum strength computation confirmed that symptomatic plaques were more hypoechoic and patchier than asymptomatic ones. This model showed an accuracy of 95.66% and can help to guide surgeons' decisions to better therapeutic strategy [99].

In another study by Sousa et al. [100], a structured hexahedral mesh using grid generation commercial software FEMAP (Siemens PLM software) was constructed to automatically evaluate three hemodynamic descriptors: the time-averaged wall shear stress, the oscillating shear index, and the relative residence time. The population study was set up of one patient with carotid stenosis >50% and one healthy control; both underwent an echocolor study to outline the vessel wall and the plaque profile and a Doppler analysis to evaluate the values of flow velocity during different phases of the cardiac cycle in the enlarged bulb and distal zone. In particular, high velocities (peak systolic velocity and

medium diastolic velocity) were detected throughout the whole area around the bulb and bifurcation in patient P1 compared with patient P2. Furthermore, higher wall shear stress values were found in the proximal tract of ICA in P1 (30–42 kPa), while lower values (22 kPa) were detected in P2 in correspondence with ECA, suggesting prevalent turbulence in the case of stenosis.

In conclusion, the automated computational fluid dynamics model was able to detect a high wall shear stress associated with carotid stenosis, particularly during the systolic phase, compared with the non-stenosis case.

In the first patient, automated computational fluid dynamics analysis detected a high wall shear stress, particularly during the systolic phase, compared with the non-stenosis case. Moreover, the method was able to identify deficiencies in Doppler velocimetry in the case of high-grade stenosis responsible for aliasing or in the case of irregular calcified plaques where artifacts hide the true lumen of the carotid artery. The limitations of the study were the rigid walls linked to the age of the patients; the possibility of errors in the estimation of flow blood patterns due to the straight flow extensions; and variability in the carotid geometry.

Intraplaque neovascularization (IPN) is another risk determinant for plaque vulnerability predisposing to lesion rupture [101,102]. IPN can be detected with contrast-enhanced ultrasound (CEUS) appearing as small contrast spots moving into and outside the atherosclerotic plaque. The intravascular localization, the small sizes of the plaques, and the presence of artifacts make IPN diagnosis difficult. For this reason, the development of methods using AI for the detection of IPN has been proposed.

Akkus et al. [103] proposed an ML software (CINQS) able to identify IPN using 45 CEUS images of carotid plaques from 29 patients. The model was able to identify the two best parameters (time-integrated IPN surface area and statistical segmentation-based IPN surface area) for the diagnosis of IPN, showing a high accuracy (AUC > 0.9) in the identification of vulnerable plaques. The limitations of the study were the use of consensus visual IPN scoring, the small size of the cohort, and the lack of histopathological confirmation.

Another factor associated with the vulnerability of atherosclerotic lesions is plaque carotid motion. In fact, during the cardiac cycle, carotid atherosclerotic plaques exhibit a multi-directional motion due to arterial displacement. Carotid motion is associated with plaque vulnerability: in particular, longitudinal displacement is responsible for a higher risk of plaque rupture than horizontal motion [104]. Different motion patterns have been described [77,105], and asynchronism between plaque and adjacent carotid walls has been linked to an increased risk of cerebrovascular events [106]. Carotid motion can be detected by radiofrequency ultrasound and B-mode with the same accuracy and reproducibility [107].

The first application of AI in the automated recognition of plaque motion as a marker of vulnerability was proposed in one study conducted by Goremati et al. B-mode ultrasound images were obtained from a cohort of 77 patients with atherosclerotic carotid disease, 18 of which were symptomatic patients with carotid stenosis of 66% ± 29%, 57 were asymptomatic with degrees of stenosis 73% ± 22%, while in 2 patients, the symptomaticity and degree of stenosis were unknown. In this study, an automated machine learning random forest (RF) algorithm was used to recognize different plaque motion patterns (evaluating the displacements inside the plaque and between the plaque and wall) and relate them to vulnerability on the basis of US echogenicity, the degree of stenosis, and symptomaticity of the plaque.

The study showed that plaque asynchronism was related to symptomaticity, echogenicity, and high-grade stenosis of plaque, proposing an accurate automated method (AUC of 0.81, 0.79, 0.89, and 0.90 for the association of plaque motion with echogenicity, symptomaticity, stenosis degree, and plaque risk, respectively) to detect vulnerable plaques for assessing stroke risk. The study was limited by the moderate size of the cohort and the heterogeneity of the dataset.

4.3. AI Based on US Images for Estimation of CVD Risk

Interestingly, deep networks have recently been applied to create automated models for the study of vascular morphology, starting from images derived from the segmentation of the media–adventitia boundary and lumen–intima boundary interface in transverse and longitudinal sections. The combination of these US images and a single-layer perceptron network preceded by an autoencoder was proposed by Menchon-Lara to estimate the intima–media thickness in an automated way [93].

Deep CNNs found application in the plaque-burden estimation of the media–adventitia boundary and lumen–intima boundary by an extensive dataset constituted of symptomatic and asymptomatic transverse carotid ultrasound images. In one study performed on a population of 15 people with different grades of carotid stenosis (between 0 and 60%), the application of a deep CNN model to examine small features from a small portion of the whole US image through the convolutional layers was used to create a fully automated approach with a good performance in the automatic measurement of the media–adventitia boundary and lumen–intima boundary (94 and 91%) [108].

AtheroEdge™ software, a fully convolutional network-based system developed according to the evaluation of the vascular contour in US images, has proven to be accurate in estimating the plaque area by tracing the distance between the lumen–intima and media–adventitia borders [109].

The sonographic study of the carotid wall is part of the assessment of cardiovascular risk. In fact, the intima–media thickening (IMT) and area of the plaque are associated with a higher cardiovascular and stroke risk. However, most of the models for risk assessment using AI have been created based on the analysis of conventional cardiovascular risk factors. Though the major application of AI based on US carotid images has been used in a diagnostic role, ML algorithms combining imaging phenotypes with or without clinical features have been proposed for the estimation of prognosis in patients with high cardiovascular risk [110].

Johri et al. [111] proposed two machine learning models (AtheroEdge-MCDL$_{AI}$: AE3.0$_{DL}$ and AtheroPoint™) correlating the carotid plaque characteristics on ultrasound study (IMT, area of plaque, maximum plaque height, and neovascularization evaluated after contrast microbubbles injection) and cardiovascular risk in 459 patients. The study demonstrated a higher performance of the ML algorithm in predicting cardio- and cerebrovascular events than conventional approaches based on clinical features. The study was limited due to the small size of the cohort, the higher baseline cardiovascular risk of the population study, and the lack of evaluation of the lipidic profile.

In conclusion, a combination of AI using DL model-based carotid ultrasound imaging frameworks and conventional risk factors may increase the accuracy in predicting cardiovascular disease compared with conventional risk calculators. Moreover, more studies validated on the use of contemporary databases are required to increase the reliability and robustness of the applicability of AI in the assessment of cardiovascular risk.

The application of artificial intelligence using US images offers a new strategy for the rapid and objective diagnosis of carotid atherosclerosis. Some limitations vitiate this new method: the performance of deep learning could be affected by the presence of noise or redundant information; the studies have been carried out on a small–moderate-sized cohort; the US images were obtained from static scans, while motion imagery has usually not been used for attempting to study intima–media thickening/atherosclerotic plaques; and semi-automated methods still require the participation of physicians.

5. Tomographic Detection of Carotid Plaque and Artificial Intelligence

The use of CT scans for carotid plaque detection included several different methods. The choice of method generally depends on the resources available and the specific needs of the clinician. Manual segmentation is the most widely used method for carotid plaque [112]. It involves a radiologist or a trained technician manually outlining the plaque in each slice of the CT scan. While this method is considered the gold standard, it is time-consuming

and can be prone to inter-observer variability. Semi-automatic segmentation involves software to automatically segment the carotid plaque and then having a radiologist or a technician verify and correct the results. This method is faster than manual segmentation and is less prone to inter-observer variability but is still time-consuming and can be affected by the quality of the CT scan [113]. Deep learning-based segmentation involves using AI algorithms to automatically segment the carotid plaque in CT scans. This method has shown promising results in recent studies and is becoming increasingly popular. It is faster and more accurate than manual and semi-automatic segmentation methods, but unfortunately, it requires a large dataset for training and can be also affected by the quality of the CT scan [114]. Finally, hybrid methods involve combining multiple methods to achieve the best results. For example, a semi-automatic segmentation method can be used to obtain the initial results, and subsequently, a deep learning-based segmentation can be applied to correct and improve the results. This method allows the best results to be achieved by combining the strengths of multiple methods [115].

The incorporation of AI algorithms in vascular imaging is an evolving area that has the potential to have a significant influence on clinical practice, helping the applicability, accuracy, and safety of tomographic acquisitions.

Multiple AI algorithms have been proposed to address a wide range of CTA pre-procedural problems [116,117], including noise reduction [117], contrast dose and radiation reduction [118,119], and image quality control [120].

It should be underlined that the vast majority of research taking advantage of AI to detect and classify atherosclerotic plaques, including their composition, was conducted on coronary atherosclerotic plaque with the purpose of developing a non-invasive coronary computed tomographic angiography, with encouraging results [121].

5.1. AI and CTA for Symptomatic Plaque

In a recent study, Buckler et al. [122] used a DL model for subtyping an atherosclerotic plaque stability phenotype on carotid CTA in comparison with histologic specimens from carotid endarterectomy. A CNN was trained to identify plaque as minimal, stable, or unstable. After training, the algorithm was validated in an unseen dataset, showing strong agreement with pathologist classification and high accuracy for each plaque phenotype recognition.

Vascular imaging plays an important role in the management of carotid artery stenosis. For example, CTA is frequently performed to confirm the diagnosis and identify the correct surgical treatment and follow-up. Several studies showed that plaque classification that includes qualitative characteristics beyond luminal stenosis could predict future cerebral ischemic events with great accuracy [123].

In this regard, radiomic characteristics were extracted from carotid CT scans in a study of patients with recent ischemic stroke to investigate their accuracy and ability to identify high-risk culprit carotid arteries from non-culprit carotid arteries. The authors combined ElasticNet logistic regression for the identification of culprit lesions using a model with 93 radiomic-derived variables with great accuracy to simulate inter-observer variability for region-of-interest demarcation, and they obtained an AUC of 0.73 [124].

Moreover, Kigka et al. developed a machine learning model to identify high-risk carotid plaques by mixing non-imaging-based characteristics and non-invasive imaging-based characteristics. An accuracy of 0.76 was achieved thanks to the relief feature selection technique and the support vector machine classification scheme [125].

In another study, the same authors [126] proposed a machine learning model for the diagnosis and detection of asymptomatic carotid artery stenosis, training the model with frequent demographics, clinical data, risk factors, and pharmacological data. The final model was able to classify the patients into high-risk (Class 1-CAS group) and low-risk (Class 0-non CAS group) individuals. The authors obtained good accuracy (0.82) and area under the curve (0.9) using the relief feature selection technique and the random forest classification scheme. Concerning carotid symptomatic plaques, a recent study assessed the

good accuracy of [AUTO]Stroke Solution large vessel occlusion (LVO) detection application in acute ischemic stroke patients [127]. Additionally, the authors compared the algorithm's accuracy with clinical experts in identifying anterior circulation occlusions. Unfortunately, a strong limitation was that no posterior circulation or medium vessel occlusion patients were considered in the study as the deep learning algorithm was extremely dependent on the training data utilized.

In a retrospective analysis [128] conducted on 610 CTAs, the performance of an AI-based algorithm for LVO detection in acute ischemic stroke was assessed. The Viz-LVO model identified occlusions of the internal carotid artery terminus and middle cerebral artery with high sensitivity (87.6%) and specificity (88.5%) and an accuracy of 87.9% (AUC 0.88, 95% CI: 0.85–0.92, $p < 0.001$). Interestingly, the mean run time of the algorithm was less than 3 min, enabling quick decision-making for reperfusion treatments.

5.2. Artificial Intelligence for Overcoming Technical Issues

Tatsugami et al. developed a CT image restoration software, MatConvNet software (ver. 1.0) based on deep learning technique incorporating a noise and artifact reduction filter using a deep convolutional neural network able to obtain the reduction of the image noise by 20% in coronary CTA [129].

Even better results were obtained by Benz et al., who evaluated a DL reconstruction model that showed an upgrade in image quality by 62% [130].

Interestingly, a recent study used CNNs to automatically detect and localize carotid plaques in cone beam computed tomography [131]. The authors used a U-Net neural network architecture to implement a neural network able to segment the image and detect calcification instances.

Visualization of the vascular system on a routine CT scan is difficult as vessels have similar radiodensities to adjacent soft tissues. Considering the contraindications and related risks, one of the future directions is to avoid contrast agent use. In this regard, DL models were adopted in order to perform a vascular high-resolution CTA without the use of a contrast agent, with promising results [132], but only a few studies have focused on carotid disease.

Olive-Gadea et al. adopted a DL-based software (MethinksLVO, Methinks Software S.L. Barcelona, Spain) to detect LVO in CT images, and they demonstrated a significant improvement in the sensitivity and specificity of LVO diagnosis [133].

Artificial intelligence application in CT scans for carotid plaque detection has the potential to revolutionize the diagnosis and treatment of carotid artery disease. However, the models applied in the current studies present both advantages and disadvantages. AI algorithms can detect even small plaques that might not be visible to the human eye, enabling earlier detection and treatment of carotid artery disease. In addition, AI algorithms can help standardize the detection of carotid plaque across different imaging centers and clinicians. However, AI algorithms depend on high-quality data for accurate detection. If the quality of the CT scan images is poor, it can lead to false positive or false negative results. Finally, there are ethical concerns surrounding the use of AI in healthcare, including issues of data privacy, bias, and accountability, which are still debated.

6. Magnetic Resonance Imaging and Artificial Intelligence

Magnetic resonance imaging (MRI) is a powerful technique for the non-invasive morphologic characterization of atherosclerotic plaques in vivo. Indeed, while other conventional instrumental technologies, such as tomographic computed angiography and ultrasonography, can detect only the size of the lesions and the alterations of the blood flow, MRI can identify the components of the plaques, allowing the vulnerability of the lesion to be estimated based on the prevalence of fibrotic and lipidic compounds and intralesional complications [134–139]. There are several methods that can be used to analyze carotid plaque using MRI. The most commonly used methods are T1-weighted imaging, T2-weighted imaging, diffusion-weighted imaging, and magnetization transfer imaging.

Each of the four methods has its strengths and weaknesses for imaging carotid plaque. The choice of imaging method should depend on the specific clinical question being addressed. MRI T1-weighted imaging provides important information for risk stratification, allowing the lipid-rich and fibrous components of the plaque to be differentiated [140]. However, T1-weighted imaging has a limited ability to detect intraplaque hemorrhage. Instead, T2-weighted imaging provides high contrast between hemorrhages and fibrous tissue within the plaque, but it has a scarce ability to differentiate lipid components. Detecting intraplaque hemorrhage represents an important predictor of plaque vulnerability [141]. Diffusion-weighted imaging (DWI) is a technique that can detect changes in the movement of water molecules within the tissue and thus has been used to assess the microstructural integrity of the plaque. In fact, DWI can detect the presence of microstructural alteration such as necrosis or fibrosis [142]. However, it has a limited ability to detect intraplaque hemorrhage. Magnetization transfer imaging (MTI) has been used to study changes in the interaction between protons within the tissue. MTI can be used to assess the extracellular matrix of the plaque, such as collagen and elastin degradation, but this technique has a limited ability to detect intraplaque hemorrhage [143].

Compared with other techniques, high-resolution MRI has some other advantages in plaque evaluation: the high-soft tissue contrast; the possibility of combining multiple contrast weightings for more valuable information; the lack of radiation; and operator independence.

High-risk plaques (HRP) are defined as plaques with luminal surface disruption or a lipid-rich necrotic core occupying >40% of the wall or intraplaque hemorrhage [144]. These characteristics most affect the risk of stroke compared to vascular lumen constriction. In this concern, recent studies have ascribed the etiology of a percentage of cryptogenic strokes to the vulnerability of carotid plaques with non-significant stenosis [58,145].

The detection of peculiar features in vessel wall–high-resolution magnetic resonance imaging (VW-HRMRI) study allows the definition of the stability of atherosclerotic plaques. Vulnerable plaques are characterized by inhomogeneous hyperintensity and irregular surfaces in the pre-enhanced MRI-T1WI sequence and hypointensity signals in the T2WI-SPAIR image, while post-enhanced T1WI vulnerability characteristics are the discontinuous thin linear enhancement on the plaque surface and hyperintensity in the plaque [146].

Recently, MRI-derived images have been used to create new software based on the use of AI to diagnose and characterize the atherosclerotic disease.

6.1. AI Application in MRI Study for Vessel Segmentation

The application of artificial intelligence in the characterization of atherosclerotic plaques consists of the creation of automated algorithms from quantitative information from magnetic resonance studies.

Computer-aided manual tracing of the vessel boundaries obtained from MRI images was the first methodology created for this purpose. A method based on "snakes" called the active contours technique [147], which is able to disclose the irregularities of the vascular profile, proved to be accurate in carotid disease research in vivo [148] and in vitro [149]. However, the operator's dependence on the outline of the contour is a limitation for the accuracy of these methods. Automated post-processing algorithms and automated segmentation networks for studying the vessel wall have been proposed to overcome this problem.

Alblas et al. [150] proposed a translationally equivariant CNN model based on 2D MRI images to obtain an automated outlining of the vascular contour. The method, based on the criteria used in the Carotid Artery Vessel Wall Segmentation Challenge [151], showed a good performance assessed by the estimation of the Dice similarity coefficient and Hausdorff distance, with the limit of the reduction of the accuracy in the case of the segmentation of horizontal segments in the vessel.

In 2004, Adame et al. [152] proposed a fully automated segmentation system to distinguish the different layers and components of atherosclerotic plaques. This algorithm

was generated from plaque contour images obtained from T1-weighted and proton density-weighted in vivo MRI and provided to the segmentation of the arterial wall using fuzzy clustering. This approach is based on the analysis in different phases to identify the three different regions (lumen, outer wall, and lipid core), identifying vulnerable plaques based on the fibrotic cap thickness and the plaque area. The study results in a valid algorithm for estimating the different degrees of stenosis in carotid arteries, confirming previous data obtained from studies in vitro [153].

Based on convolutional neural networks, Wu et al. [154] proposed a deep morphology-aided diagnosis (DeepMAD) network for the early diagnosis of carotid atherosclerosis using the black-blood vessel wall–MRI study. One thousand and fifty-seven carotid MRI scans from the CAREII dataset [140] were collected and used to create automated software for carotid wall segmentation. DeepMAD comprises two parts, the segmentation subnetwork and the diagnosis subnetwork. The presence of two datasets improves the software performance, providing the automated diagnosis of atherosclerotic disease based on tracing the lumen and outer wall areas, with comparable results with the manual marking of the wall boundaries.

Recently, a 3D meshed model of the carotid bifurcation and smaller branches was proposed [155]. The model results from implementing a U-net-based CNN algorithm through the combination of active morphological contours by iterative frameworks. Multi-spectral magnetic resonance imaging series images of the carotid circle of patients selected in the TAXINOMISIS study [156] were used for the 3D reconstruction of the carotid vascular tree. This approach overcomes the limit of manual segmentation, making available an accurate and automated model. Despite the initial promising results, the model must be fully validated in larger datasets.

6.2. MRI-Applied AI for the Estimation of the Vulnerability of the Plaque

Most studies involving the application of AI for determining plaque vulnerability were carried out on ultrasound and tomography-computed angiography techniques, while data obtained from MRI studies are very few. Scarce data about the use of AI algorithms from magnetic resonance images for classifying atherosclerotic plaques are encountered in the literature.

6.2.1. MRI in Intracranial Plaque

In a retrospective study performed in 2018 [157], patients with intracranial stenosis who underwent intracranial MRI using a 3-T whole-body MRI scanner (Skyra; Siemens Healthcare, Erlangen, Germany) between January 2014 and December 2016 were selected with the aim of correlating the basilar plaque characteristics and symptomatic evolution. A dedicated software (3D-Slicer) analyzed 94 radiomic features—including intensity (maximal intensity, mean intensity, and standard deviation of intensity), shape-based features (area, length, etc.), and textures—obtained from the MRI images. Among these, only seven radiomic features in T1 images and three in contrast-enhanced (CE)-T1 images were independently associated with acute/sub-acute symptoms. In contrast, none of the features in T2 images was statistically significant in the final random forest analysis. The combination of radiomic features from T1 and CE-T1 images provides a system with a sensitivity, specificity, and accuracy of 97.0, 79.0, and 83.2%, respectively, resulting in improved accuracy of the stroke risk assessment. Unfortunately, the study was conditioned by some limitations, such as the small size sample, the use of 2D imaging data, and manual segmentation for the plaque boundary.

Afterward, Shi et al. [158] proposed a histogram texture analysis for distinguishing vulnerable and stable plaques in middle cerebral and basilar arteries, resulting in a higher coefficient of variation (CV) on T1WIs in vulnerable plaques than the stable ones. The variation of CV, only in the T1WI sequence, may be linked to the higher variation signal intensity on this sequence in the case of intraplaque hemorrhage, a lipid-rich necrotic core, calcification, and fibrous tissue components in plaques.

6.2.2. MRI in Carotid Plaque

More recently, Zhang et al. [159] conducted a study on a cohort of 162 patients with symptomatic and asymptomatic carotid plaques. Patients were considered symptomatic if an acute stroke or transitory ischemic attack was recently diagnosed. All the patients underwent an MRI study to evaluate the carotid arteries using a 3-T MR scanner (MAGNE-TOM Verio, Siemens Healthineers) with a 16-channel head coil and an 8-channel carotid coil. Afterward, MRI images were analyzed using an open-source software ITK-SNAP version 3.8.0 using the least absolute shrinkage and selection operator (LASSO) algorithm for automated plaque segmentation. The multi-variable logistic regression analysis found 33 features to build a high-risk plaque MRI-based model (HRPMM) for estimating a risk score linked to plaque vulnerability in an automated way. The strength of the results was dampened by some limits: a small sample size, the not fully automated determination of ROIs (regions of interest), the inclusion of only two radiological characteristics (intraplaque hemorrhage and a lipid-rich necrotic core), and the radiomic analysis executed on the slice with the largest plaque area due to time restrictions, which prevented the use of the 3D analysis.

The results obtained from the abovementioned studies suggest that MRI-based radiomic methods can find more differential features useful to characterize plaque stability than the subjective operator's evaluation. However, considering the limitations of the reported studies, the available data are limited, and prospective studies are required to provide more valuable information in the future and validate the models' ability to predict the risk of stroke.

7. New Technologies and Future Perspectives

The use of artificial intelligence to improve the accuracy and speed of recognition of symptomatic carotid plaque is increasing. Consequently, new ML and DL algorithms have increasingly been combined with more advanced diagnostic tools. This synergic union could allow the diagnostic potential of new emerging technologies to be increased.

7.1. Late-Phase CEUS

In ultrasound imaging, the application of late-phase CEUS has been proposed as a technique to directly detect inflammatory elements, and it is performed by imaging the artery minutes after the injection of microbubbles. These microbubbles are small gas-filled bubbles that are injected intravenously and act as ultrasound contrast agents. The microbubbles are designed to remain in the bloodstream and not cross the blood–brain barrier, making them safe for carotid imaging [160]. The analysis of late-phase CEUS images involves the use of semi-quantitative and qualitative techniques. The semi-quantitative technique involves measuring the degree and duration of contrast enhancement within the plaque using a region of interest (ROI) analysis. The qualitative technique involves visual assessment of the contrast enhancement pattern within the plaque, such as the presence of neovascularization or intraplaque hemorrhage [160].

The primary aim of the study of late-CEUS is to give time for its clearance and detect the remaining signal in the lumen, which is suggestive of contrast tissue retention probably due to two factors: (i) the phagocytosis of microbubbles by monocytes [161] and (ii) the adhesion of microbubbles to the damaged surface of the endothelium [162,163]. Nanotechnology and nanomedicine have recently been identified as suitable medical imaging techniques using nanoparticles. These extremely small particles, ranging in size from 1 to 100 nanometers, can bind to specific biomolecules found in carotid plaque, such as matrix metalloproteinases (MMPs) or oxidized low-density lipoproteins (LDLs) [164]. Nanoparticles can be designed to emit a fluorescent signal when they bind to their target, allowing the non-invasive imaging of the plaque. Researchers have also developed contrast agents based on nanoparticles, such as iron oxide nanoparticles, that can be targeted to specific biomolecules in carotid plaque. These contrast agents can be visualized using magnetic resonance imaging (MRI), allowing high-resolution images of the plaque. The

biomolecules can be precisely controlled in terms of their properties and structure and can then serve as imaging contrast agents because of the possibility to label them in accordance to the used technique: Gd^{3+} and Fe^{3+} for MRI; Au for X-ray and CT imaging; ^{64}Cu for PET and ^{111}In for SPECT imaging; and fluorophores and quantum dots for optical imaging or surfaces that can be modified with antibodies or ligands which the target receptors over overexpressed on the surface/inside of atherosclerotic plaques [165,166].

7.2. Optical Coherence Tomography

Optical coherence tomography (OCT) is a non-invasive imaging technique used to capture high-resolution images of biological tissues, such as the retina in the eye. It works by measuring the echoes of light waves as they reflect off different layers of tissue. OCT uses a low-power light source, typically in the near-infrared range, to produce images that have a resolution of a few micrometers. The light is directed onto the tissue, and then the echoes of the light waves that bounce back are analyzed to create a detailed image of the tissue. OCT generates images by measuring the backscattered light from the tissue using a Michelson interferometer. The light source emits near-infrared light, which penetrates the tissue and is backscattered by the tissue structures. Finally, the backscattered light is collected by the probe and then processed by the interferometer to generate a 2D or 3D image of the tissue [167].

A recent study [168] used OCT images to evaluate the characteristics of plaque and create a scale together with clinical indicators and digital subtraction angiography to pinpoint symptomatic plaque features.

7.3. Positron Emission Tomography/Computed Tomography

Positron emission tomography/computed tomography (PET/CT) with ^{18}F-sodium fluoride (NaF) is an innovative imaging technique that has been used to identify arterial wall micro-calcification before macro-calcification can be detected by ultrasound, CTA, or MRI. It is based on the accumulation of 18F-NaF at sites of active calcification within atherosclerotic plaques. NaF-PET/CT has been shown to be a promising imaging modality for the detection of vulnerable plaques in the carotid arteries, which are associated with a higher risk of stroke. The technical details of NaF-PET/CT involve the injection of a small amount of 18F-NaF into the patient's bloodstream. The NaF-PET/CT scan is then performed after a short waiting period to allow the 18F-NaF to accumulate in the atherosclerotic plaques. The PET scan measures the amount of 18F-NaF that has accumulated in the plaque, while the CT scan provides a detailed anatomical image of the carotid arteries.

Piri et al. [169] used CCN-based segmentation obtaining faster standardized uptake mean values with the same accuracy of human operators. The abovementioned new technologies represent some of the most modern tools for the recognition of symptomatic carotid atherosclerosis. Thus, the combination of AI with these technologies could provide new important information about correct risk plaque classifications.

8. Discussion

AI has shown great promise in improving the accuracy and efficiency of medical imaging interpretation. In recent years, there has been an increasing interest in the application of AI in carotid plaque detection using ultrasound, CT scans, and MRI. U-Net, a CNN model that uses contracting and up-sampling layers with skip connections, has been used for carotid segmentation with high accuracy (Dice coefficient 0.9) in a study by Zhou et al. [88] (see Table S1). Dilated U-Net, which combines U-Net with dilated convolution networks, has shown a better performance than U-Net alone in complex plaques [91]. However, semi-automated segmentation is required in dilated U-Net, which presents some limitations. Furthermore, the study by Jain et al. has shown good accuracy in carotid wall segmentation using deep learning U-Net architecture for two different demographic groups of patients [97]. CNN-based models and U-Net have also been used to classify carotid plaques into vulnerable and stable lesions [21]. Interestingly, the optimized system,

DCNN11A5, has been proposed for computed plaque characterization, distinguishing symptomatic and asymptomatic plaque with higher accuracy than other machine learning methods [99] (see Table S1).

As this review demonstrates, the use of artificial intelligence in vascular imaging is an area of growing interest that has the potential to significantly impact clinical practice by improving the applicability, accuracy, and safety of tomographic acquisitions [116]. Multiple AI algorithms have been proposed to address various CTA pre-procedural problems, such as noise reduction, contrast dose and radiation reduction, and image quality control [117–120]. Unsurprisingly, the majority of research using AI to detect and classify atherosclerotic plaques has been conducted on coronary atherosclerotic plaque, with promising results for the development of a non-invasive coronary computed tomographic angiography [121]. In a recent study, Buckler et al. used a deep learning (DL) model to subtype atherosclerotic plaque stability phenotypes on carotid CTA and showed strong agreement with pathologist classification and high accuracy for each plaque phenotype recognition [122]. Other studies have demonstrated the potential of AI and CTA for the management of carotid artery stenosis, such as plaque classification beyond luminal stenosis to predict future cerebral ischemic events [123] (see Table S2). Additionally, radiomic characteristics were extracted from carotid CT scans to identify high-risk culprit carotid arteries from non-culprit carotid arteries [124]. Kigka et al. developed a machine learning model to identify high-risk carotid plaques and achieved an accuracy of 0.76 [125]. They also proposed a machine learning model for the diagnosis and detection of asymptomatic carotid artery stenosis and obtained good accuracy and area under the curve [126] (see Table S2). Furthermore, DL algorithms have shown good accuracy in the detection of large vessel occlusions in acute ischemic stroke patients [127,128]. AI has also been used to overcome technical issues in vascular imaging, such as image noise and artifact reduction [129], reconstruction model improvement [130], the automatic detection and localization of carotid plaques [131], and high-resolution CTA without contrast agent use [132]. Olive-Gadea et al. used DL-based software (MethinksLVO, Methinks Software S.L. Barcelona, Spain) to detect LVO in CT images and demonstrated a significant improvement in sensitivity and specificity for LVO diagnosis [133]. Overall, the use of AI in vascular imaging holds great promise for improving clinical outcomes and enhancing patient care. However, further research is needed to validate and refine these approaches for routine clinical use. In addition, this review underlines the advantages of using high-resolution MRI in plaque evaluation, including high soft-tissue contrast, the ability to combine multiple contrast weightings, lack of radiation, and operator independence. It highlights the importance of identifying high-risk plaques, which are defined by certain characteristics, including luminal surface disruption, intraplaque hemorrhage, and a lipid-rich necrotic core. Recent studies have suggested that vulnerable carotid plaques with non-significant stenosis may contribute to cryptogenic strokes [145]. Several studies have evaluated the effectiveness of AI in the segmentation of the vessel wall and estimation of the vulnerability of plaque using MRI [146,148,149] (see Table S3). The studies show promising results, such as a good performance in the estimation of the Dice similarity coefficient and Hausdorff distance. However, the methods need to be validated in larger datasets. While the application of AI in ultrasound, CT scans, and MRI for various medical applications shows great promise, there are several major issues that need to be addressed before these approaches can be adopted on a large scale in clinical practice. The first issue is data availability and quality. In fact, AI algorithms require large amounts of high-quality data to be trained effectively. In many cases, the amount and quality of available medical imaging data may be limited, and obtaining more data can be difficult and expensive. Secondly, AI algorithms trained on data from one population may not perform as well on data from other populations due to differences in imaging protocols, patient demographics, and disease prevalence. Furthermore, many AI algorithms are "black boxes," meaning that they are difficult to interpret or understand how they make their predictions. This can be a concern for clinicians who need to make treatment decisions based on AI-generated results. Nevertheless, the

use of AI in medical imaging raises important regulatory and ethical issues, such as data privacy, liability, and patient consent. These issues need to be addressed before AI-based approaches can be adopted on a large scale in clinical practice. Moreover, to be effective, AI-based approaches need to be integrated seamlessly into existing clinical workflows. This requires close collaboration between AI researchers and clinical stakeholders, as well as the development of user-friendly interfaces and tools for clinicians. Overall, addressing these issues will be critical for the successful adoption of AI-based approaches in medical imaging, including ultrasound, CT scans, and MRI, in clinical practice.

9. Conclusions

This review provides a useful guide for both readers who are approaching artificial intelligence algorithms in the field of carotid atherosclerosis for the first time and for researchers who intend to apply some of the algorithms presented or are interested in creating their own. AI has been demonstrated to be a valid help in identifying the characteristics of vulnerable and potentially symptomatic plaque, increasing the accuracy of imaging detection, or simply speeding up the diagnostic process. In particular, the application of AI using US, CTA, and MRI images offers a new strategy for the rapid and objective diagnosis of carotid atherosclerosis. Unfortunately, some characteristics limit widespread use in clinical practice: the moderate size of the cohorts in most of the studies represents a huge limit for the correct training of deep learning models; the performance of deep learning could be affected by the presence of noise or redundant information; the US images were obtained from static scans, while motion imagery has not usually been used for attempting to study intima–media thickening/atherosclerotic plaques; semi-automated methods still require the participation of physicians; there are scarce data combining imaging and biohumoral markers; and difficulties in the comprehension of complex model results by end-users (physicians) is still one of the main issues. Considering the limitations of the reported studies, the available data are limited, and prospective studies are required to provide more valuable information in the future and validate the models' ability to predict the risk of stroke. In particular, the use of AI in CT scans for carotid plaque detection offers many potential benefits, but the abovementioned limitations and ethical concerns need to be addressed to ensure appropriate and effective use in clinical practice. Thus, more multi-center, large-scale, and prospective studies, and above all, some considering MRI techniques, must be carried out to validate the role of AI in symptomatic carotid plaque detection.

Abbreviations

AHA	American Heart Association
AI	artificial intelligence
ANNS	artificial neural network architectures
CAS	carotid artery stenosis
CEUS	contrast-enhanced ultrasound
CNN	convolutional neural network
CT	computed tomography
CTA	computed tomographic angiography
CV	coefficient of variation
DL	deep learning
ESC	European Society of Cardiology
GRUS	gated recurrent units
LAAS	large artery atherosclerosis
LASSO	least absolute shrinkage and selection operator
LVO	large vessel occlusion
ML	machine learning
MRI	magnetic resonance imaging
OCT	optical coherence tomography
PET	positron emission tomography
RNN	recurrent neural networks
SPECT	single photon emission computed tomography
SVMs	support vector machines
TF	tissue factor
TIA	transient ischemic attack
TOAST	Trial of Org 10172 in Acute Stroke Treatment
US	ultrasound
VW-HRMRI	vessel wall–high-resolution magnetic resonance imaging

References

1. Zhu, W.; Churilov, L.; Campbell, B.C.V.; Lin, M.; Liu, X.; Davis, S.M.; Yan, B. Does large vessel occlusion affect clinical outcome in stroke with mild neurologic deficits after intravenous thrombolysis? *J. Stroke Cerebrovasc. Dis.* **2014**, *23*, 2888–2893. [CrossRef] [PubMed]
2. Smith, W.S.; Tsao, J.W.; Billings, M.E.; Johnston, S.C.; Hemphill, J.C., 3rd; Bonovich, D.C.; Dillon, W.P. Prognostic Significance of angiographically confirmed large vessel intracranial occlusion in patients presenting with acute brain ischemia. *Neurocrit. Care* **2006**, *4*, 14–17. [CrossRef] [PubMed]
3. Smith, W.S.; Lev, M.H.; English, J.D.; Camargo, E.C.; Chou, M.; Johnston, S.C.; Gonzalez, G.; Schaefer, P.W.; Dillon, P.D.; Koroshetz, W.J.; et al. Significance of large vessel intracranial occlusion causing acute ischemic stroke and TIA. *Stroke* **2009**, *40*, 3834–3840. [CrossRef]
4. Brott, T.G.; Halperin, J.L.; Abbara, S.; Bacharach, J.M.; Barr, J.D.; Bush, R.L.; Cates, C.U.; Creager, M.A.; Fowler, S.B.; Friday, G.; et al. Guideline on the management of patients with extracranial carotid and vertebral artery disease. *J. Am. Coll. Cardiol.* **2011**, *57*, 516–594. [CrossRef] [PubMed]
5. Jovanović, Z.B.; Pavlović, M.A.; Vujisić Tešić, P.B.; Kostić, V.M.B.; Cvitan, Z.E.; Pekmezović, P.T.; Šternić Čovičković, M.N. The Significance of the ultrasound diagnostics in evaluation of the emboligenic pathogenesis of transient ischemic attacks. *Ultrasound Med. Biol.* **2013**, *39*, 597–603.
6. Sirimarco, G.; Amarenco, P.; Labreuche, J.; Touboul, P.J.; Alberts, M.; Goto, S.; Rother, J.; Mas, J.L.; Bhatt, D.L.; Steg, P.G. Carotid atherosclerosis and risk of subsequent coronary event in outpatients with atherothrombosis. *Stroke* **2013**, *44*, 373–379. [CrossRef] [PubMed]
7. Berkhemer, O.A.; Fransen, P.S.; Beumer, D.; van den Berg, L.A.; Lingsma, H.F.; Yoo, A.J.; Schonewille, W.J.; Vos, J.A.; Nederkoorn, P.J.; Wermer, M.J.H.; et al. A randomized trial of intraarterial treatment for acute ischemic stroke. *N. Engl. J. Med.* **2015**, *372*, 11–20. [CrossRef]

8.   Goyal, M.; Demchuk, A.M.; Menon, B.K.; Eesa, M.; Rempel, J.L.; Thornton, J.; Roy, D.; Jovin, T.G.; Willinsky, R.A.; Sapkota, B.L.; et al. Randomized assessment of rapid endovascular treatment of ischemic stroke. *N. Engl. J. Med.* **2015**, *372*, 1019–1030. [CrossRef]

9.   Jovin, T.G.; Chamorro, A.; Cobo, E.; de Miquel, M.A.; Molina, C.A.; Rovira, A.; San Román, L.; Serena, J.; Abilleira, S.; Ribó, M.; et al. Thrombectomy within 8 hours after symptom onset in ischemic stroke. *N. Engl. J. Med.* **2015**, *372*, 2296–2306. [CrossRef] [PubMed]

10. Bracard, S.; Ducrocq, X.; Mas, J.L.; Soudant, M.; Oppenheim, C.; Moulin, T.F. Mechanical thrombectomy after intravenous alteplase versus alteplase alone after stroke (THRACE): A randomized controlled trial. *Lancet Neurol.* **2016**, *15*, 1138–1147. [CrossRef]

11. Mocco, J.; Zaidat, O.O.; von Kummer, R.; Yoo, A.J.; Gupta, R.; Lopes, D.; Frei, D.; Shownkeen, H.; Budzik, R.; Ajani, Z.A.; et al. Aspiration thrombectomy after intravenous alteplase versus intravenous alteplase alone. *Stroke* **2016**, *47*, 2331–2338. [CrossRef] [PubMed]

12. Muir, K.W.; Ford, G.A.; Messow, C.M.; Ford, I.; Murray, A.; Clifton, A.; Brown, M.M.; Madigan, J.; Lenthall, R.; Robertson, F.; et al. Endovascular therapy for acute ischaemic stroke: The Pragmatic Ischaemic Stroke Thrombectomy Evaluation (PISTE) randomized, controlled trial. *J. Neurol. Neurosurg. Psychiatry* **2017**, *88*, 38–44. [CrossRef] [PubMed]

13. Campbell, B.C.V.; Donnan, G.A.; Lees, K.R.; Hacke, W.; Khatri, P.; Hill, M.D.; Goyal, M.; Mitchell, P.J.; Saver, J.L.; Diener, H.C.; et al. Endovascular stent thrombectomy: The new standard of care for large vessel ischaemic stroke. *Lancet Neurol.* **2015**, *14*, 846–854. [CrossRef] [PubMed]

14. Saver, J.L. Time is brain–quantified. *Stroke* **2006**, *37*, 263–266. [CrossRef] [PubMed]

15. Meijers, W.C.; de Boer, R.A. Common risk factors for heart failure and cancer. *Cardiovasc. Res.* **2019**, *115*, 844–853. [CrossRef] [PubMed]

16. Porcu, M.; Mannelli, L.; Melis, M.; Suri, J.S.; Gerosa, C.; Cerrone, G.; Defazio, G.; Faa, G.; Saba, L. Carotid plaque imaging profiling in subjects with risk factors (diabetes and hypertension). *Cardiovasc. Diagn. Ther.* **2020**, *10*, 1005–1018. [CrossRef] [PubMed]

17. Saba, L.; Sanagala, S.S.; Gupta, S.K.; Koppula, V.K.; Johri, A.M.; Khanna, N.N.; Mavrogeni, S.; Laird, J.R.; Pareek, G.; Miner, M.; et al. Multimodality carotid plaque tissue characterization and classification in the artificial intelligence paradigm: A narrative review for stroke application. *Ann. Transl. Med.* **2021**, *9*, 1206. [CrossRef] [PubMed]

18. Shafaat, O.; Bernstock, J.D.; Shafaat, A.; Yedavalli, V.S.; Elsayed, G.; Gupta, S.; Sotoudeh, E.; Sair, H.I.; Yousem, D.M.; Sotoudeh, H. Leveraging artificial intelligence in ischemic stroke imaging. *J. Neuroradiol.* **2022**, *49*, 343–351. [CrossRef]

19. Faes, L.; Liu, X.; Wagner, S.K.; Fu, D.J.; Balaskas, K.; Sim, D.A.; Bachmann, L.M.; Keane, P.A.; Denniston, A.K. A Clinician's Guide to Artificial Intelligence: How to Critically Appraise Machine Learning Studies. *Transl. Vis. Sci. Technol.* **2020**, *9*, 7. [CrossRef]

20. Yu, K.H.; Beam, A.L.; Kohane, I.S. Artificial intelligence in healthcare. *Nat. Biomed. Eng.* **2018**, *2*, 719–731. [CrossRef]

21. Krizhevsky, A.; Sutskever, I.; Hinton, G.E. ImageNet Classification with Deep Convolutional Neural Networks. *Commun. ACM* **2017**, *60*, 84–90. [CrossRef]

22. Hinton, G. Deep Learning-A Technology with Potential to Transform Health Care. *JAMA* **2018**, *320*, 1101–1102. [CrossRef] [PubMed]

23. Choi, R.Y.; Coyner, A.S.; Kalpathy-Cramer, J.; Chiang, M.F.; Campbell, J.P. Introduction to Machine Learning, Neural Networks, and Deep Learning. *Transl. Vis. Sci. Technol.* **2020**, *9*, 14.

24. Bonkhoff, A.K.; Grefkes, C. Precision medicine in stroke: Towards personalized outcome predictions using artificial intelligence. *Brain* **2022**, *145*, 457–475. [CrossRef] [PubMed]

25. Kamari, Y.; Werman-Venkert, R.; Shaish, A.; Harari, A.; Gonen, A.; Voronov, E.; Grosskopf, I.; Sharabi, Y.; Grossman, E.; Iwakura, Y.; et al. Differential role and tissue specificity of interleukin-1alpha gene expression in atherogenesis and lipid metabolism. *Atherosclerosis* **2007**, *195*, 31–38. [CrossRef]

26. Morton, A.C.; Rothman, A.M.; Greenwood, J.P.; Gunn, J.; Chase, A.; Clarke, B.; Hall, A.S.; Fox, K.; Foley, K.; Banya, W.; et al. The effect of interleukin-1 receptor antagonist therapy on markers of inflammation in non-ST elevation acute coronary syndromes: The MRC-ILA heart study. *Eur. Heart J.* **2015**, *36*, 377–384. [CrossRef]

27. Abbate, A.; Trankle, C.R.; Buckley, L.F.; Lipinski, M.J.; Appleton, D.; Kadariya, D.; Canada, J.M.; Carbone, S.; Roberts, C.S.; Abouzaki, N.; et al. Interleukin-1 blockade inhibits the acute inflammatory response in patients with ST-segment-elevation myocardial infarction. *J. Am. Heart Assoc.* **2020**, *9*, e014941. [CrossRef]

28. Mallat, Z.; Corbaz, A.; Scoazec, A.; Graber, P.; Alouani, S.; Esposito, B.; Humbert, Y.; Chvatchko, Y.; Tedgui, A. Interleukin-18/interleukin-18 binding protein signaling modulates atherosclerotic lesion development and stability. *Circ. Res.* **2001**, *89*, E41–E45. [CrossRef]

29. Zhang, J.; Alcaide, P.; Liu, L.; Sun, J.; He, A.; Luscinskas, F.W.; Shi, G.P. Regulation of endothelial cell adhesion molecule expression by mast cells, macrophages, and neutrophils. *PLoS ONE* **2011**, *6*, e14525. [CrossRef]

30. Zanoli, L.; Briet, M.; Empana, J.P.; Cunha, P.G.; Mäki-Petäjä, K.M.; Protogerou, A.D.; Tedgui, A.; Touyz, R.M.; Schiffrin, E.L.; Spronck, B.; et al. Association for Research into Arterial Structure, Physiology (ARTERY) Society, the European Society of Hypertension (ESH) Working Group on Vascular Structure and Function, and the European Network for Noninvasive Investigation of Large Arteries. Vascular consequences of inflammation: A position statement from the ESH Working Group on Vascular Structure and Function and the ARTERY Society. *J. Hypertens.* **2020**, *38*, 1682–1698.

31. Birck, M.M.; Saraste, A.; Hyttel, P.; Odermarsky, M.; Liuba, P.; Saukko, P.; Hansen, A.K.; Pesonen, E. Endothelial cell death and intimal foam cell accumulation in the coronary artery of infected hypercholesterolemic minipigs. *J. Cardiovasc. Transl. Res.* **2013**, *6*, 579–587. [CrossRef] [PubMed]

32. Wang, L.; Ai, Z.; Khoyratty, T.; Zec, K.; Eames, H.L.; van Grinsven, E.; Hudak, A.; Morris, S.; Ahern, D.; Monaco, C.; et al. ROS-producing immature neutrophils in giant cell arteritis are linked to vascular pathologies. *JCI Insight* **2020**, *5*, e139163. [CrossRef]

33. Warnatsch, A.; Ioannou, M.; Wang, Q.; Papayannopoulos, V. Neutrophil extracellular traps license macrophages for cytokine production in atherosclerosis. *Science* **2015**, *349*, 316–320. [CrossRef] [PubMed]

34. Ketelhuth, D.F.J.; Hansson, G.K. Adaptive response of T and B cells in atherosclerosis. *Circ. Res.* **2016**, *118*, 668–678. [CrossRef] [PubMed]

35. Saigusa, R.; Winkels, H.; Ley, K. T cell subsets and functions in atherosclerosis. *Nat. Rev. Cardiol.* **2020**, *17*, 387–401. [CrossRef]

36. Subramanian, M.; Tabas, I. Dendritic cells in atherosclerosis. *Semin. Immunopathol.* **2014**, *36*, 93–102. [CrossRef]

37. Nus, M.; Sage, A.P.; Lu, Y.; Masters, L.; Lam, B.Y.H.; Newland, S.; Weller, S.; Tsiantoulas, D.; Raffort, J.; Marcus, D.; et al. Marginal zone B cells control the response of follicular helper T cells to a high-cholesterol diet. *Nat. Med.* **2017**, *23*, 601–610. [CrossRef]

38. Olie, R.H.; van der Meijden, P.E.J.; Ten Cate, H. The coagulation system in atherothrombosis: Implications for new therapeutic strategies. *Res. Pract. Thromb. Haemost.* **2018**, *2*, 188–198. [CrossRef]

39. Borissoff, J.I.; Heeneman, S.; Kilinç, E.; Kassák, P.; Van Oerle, R.; Winckers, K.; Govers-Riemslag, J.W.P.; Hamulyák, K.; Hackeng, T.M.; Daemen, M.J.A.P.; et al. Early Atherosclerosis Exhibits an Enhanced Procoagulant State. *Circulation* **2010**, *122*, 821–830. [CrossRef]

40. Westmuckett, A.D.; Lupu, C.; Goulding, D.A.; Das, S.; Kakkar, V.V.; Lupu, F. In situ analysis of tissue factor-dependent thrombin generation in human atherosclerotic vessels. *Thromb. Haemost.* **2000**, *84*, 904–911. [CrossRef]

41. Cooper, B.A.; Penne, E.L.; Bartlett, L.H.; Pollock, C.A. Protein malnutrition and hypoalbuminemia as predictors of vascular events and mortality in ESRD. *Am. J. Kidney Dis.* **2004**, *43*, 61–66. [CrossRef] [PubMed]

42. Ardissino, D.; Merlini, P.A.; Bauer, K.A.; Bramucci, E.; Ferrario, M.; Coppola, R.; Fetiveau, R.; Lucreziotti, S.; Rosenberg, R.D.; Mannucci, P.M. Thrombogenic potential of human coronary atherosclerotic plaques. *Blood* **2001**, *98*, 2726–2729. [CrossRef]

43. Hollenberg, M.D.; Saifeddine, M.; Al-Ani, B.; Guy, Y. Proteinase-activated receptor 4 (PAR4): Action of PAR4-activating peptidesin vascular and gastric tissue and lack of cross-reactivity withPAR1 and PAR2. *Can. J. Physiol. Pharmacol.* **1999**, *77*, 458–464. [CrossRef] [PubMed]

44. Emilsson, K.; Wahlestedt, C.; Sun, M.K.; Nystedt, S.; Owman, C.; Sundelin, J. Vascular effects of proteinase-activated receptor 2 ago-nist peptide. *J. Vasc. Res.* **1997**, *34*, 267–272. [CrossRef] [PubMed]

45. Fernandez, D.M.; Rahman, A.H.; Fernandez, N.F.; Chudnovskiy, A.; Amir, E.A.D.; Amadori, L.; Khan, N.S.; Wong, C.K.; Shamailova, R.; Hill, C.A.; et al. Single-cell immune landscape of human atherosclerotic plaques. *Nat. Med.* **2019**, *25*, 1576–1588. [CrossRef] [PubMed]

46. Moore, K.J.; Sheedy, F.J.; Fisher, E.A. Macrophages in atherosclerosis: A dynamic balance. *Nat. Rev. Immunol.* **2013**, *13*, 709–721. [CrossRef]

47. Sage, A.P.; Tsiantoulas, D.; Binder, C.J.; Mallad, Z. The role of b cells in atherosclerosis. *Nat. Rev. Cardiol.* **2019**, *16*, 180–196. [CrossRef]

48. Wang, J.; Kang, Z.; Liu, Y.; Li, Z.; Liu, Y.; Liu, J. Identification of immune cell infiltration and diagnostic biomarkers in unstable atherosclerotic plaques by integrated bioinformatics analysis and machine learning. *Front. Immunol.* **2022**, *13*, 956078. [CrossRef]

49. Hetterich, H.; Webber, N.; Willner, M.; Herzen, J.; Birnbacher, L.; Hipp, A.; Marschner, M.; Auweter, S.D.; Habbel, C.; Schüller, U.; et al. AHA classification of coronary and carotid atherosclerotic plaques by grating-based phase-contrast computed tomography. *Eur. Radiol.* **2016**, *26*, 3223–3233. [CrossRef]

50. Miceli, G.; Basso, M.G.; Rizzo, G.; Pintus, C.; Tuttolomondo, A. The Role of the Coagulation System in Peripheral Arterial Disease: Interactions with the Arterial Wall and Its Vascular Microenvironment and Implications for Rational Therapies. *Int. J. Mol. Sci.* **2022**, *23*, 14914. [CrossRef]

51. North American Symptomatic Carotid Endarterectomy Trial. Methods, patient characteristics, and progress. *Stroke* **1991**, *22*, 711–720. [CrossRef] [PubMed]

52. Bonati, L.H.; Kakkos, S.; Berkefeld, J.; de Borst, G.J.; Bulbulia, R.; Halliday, A.; van Herzeele, I.; Koncar, I.; McCabe, D.J.; Lal, A.; et al. European Stroke Organisation guideline on endarterectomy and stenting for carotid artery stenosis. *Eur. Stroke J.* **2021**, *6*, I-XLVII. [CrossRef]

53. Mechtouff, L.; Rascle, L.; Crespy, V.; Canet-Soulas, E.; Nighoghossian, N.; Millon, A. A narrative review of the pathophysiology of ischemic stroke in carotid plaques: A distinction versus a compromise between hemodynamic and embolic mechanism. *Ann. Transl. Med.* **2021**, *9*, 1208. [CrossRef] [PubMed]

54. Carballo-Perich, L.; Puigoriol-Illamola, D.; Bashir, S.; Terceño, M.; Silva, Y.; Gubern-Mérida, C.; Serena, J. Clinical Parameters and Epigenetic Biomarkers of Plaque Vulnerability in Patients with Carotid Stenosis. *Int. J. Mol. Sci.* **2022**, *23*, 5149. [CrossRef]

55. Naylor, A.R.; Ricco, J.B.; de Borst, G.J.; Debus, S.; de Haro, J.; Halliday, A.; Hamilton, G.; Kakisis, J.; Kakkos, S.; Lepidi, S.; et al. Management of atherosclerotic carotid and vertebral artery disease: 2017 clinical practice guidelines of the European society for vascular surgery (ESVS). *Eur. J. Vasc. Endovasc.* **2017**, *55*, 142–143. [CrossRef] [PubMed]

56. Ferguson, G.G.; Eliasziw, M.; Barr, H.W.; Clagett, G.P.; Barnes, R.W.; Wallace, M.C.; Taylor, D.W.; Haynes, R.B.; Finan, J.W.; Hachinski, V.C.; et al. The North American Symptomatic Carotid Endarterectomy Trial: Surgical results in 1415 patients. *Stroke* **1999**, *30*, 1751–1758. [CrossRef] [PubMed]

57. European Carotid Surgery Trialists' Collaborative Group. Randomised trial of endarterectomy for recently symptomatic carotid stenosis: Final results of the MRC European Carotid Surgery Trial (ECST). *Lancet* **1998**, *351*, 1379–1387. [CrossRef]

58. Hyafil, F.; Schindler, A.; Sepp, D.; Obenhuber, T.; Bayer-Karpinska, A.; Boeckh-Behrens, T.; Höhn, S.; Hacker, M.; Nekolla, S.G.; Rominger, A.; et al. High-risk plaque features can be detected in non-stenotic carotid plaques of patients with ischaemic stroke classified as cryptogenic using combined (18)F-FDG PET/MR imaging. *Eur. J. Nucl. Med. Mol. Imaging* **2016**, *43*, 270–279. [CrossRef]

59. Aboyans, V.; Ricco, J.B.; Bartelink, M.E.L.; Björck, M.; Brodmann, M.; Cohnert, T.; Collet, J.P.; Czerny, M.; De Carlo, M.; Debus, S.; et al. 2017 ESC guidelines on the diagnosis and treatment of peripheral arterial diseases, in collaboration with the European society for vascular surgery (ESVS): Document covering atherosclerotic disease of extracranial carotid and vertebral, mesenteric, renal, upper and lower extremity arteries Endorsed by: The European stroke organization (ESO) the task force for the diagnosis and treatment of peripheral arterial diseases of the European society of Cardiology (ESC) and of the European society for vascular surgery (ESVS). *Eur. Heart J.* **2018**, *39*, 763–816.

60. Saba, L.; Yuan, C.; Hatsukami, T.S.; Balu, N.; Qiao, Y.; DeMarco, J.K.; Saam, T.; Moody, A.R.; Li, D.; Matouk, C.C.; et al. Carotid artery wall imaging: Perspective and guidelines from the ASNR vessel wall imaging study group and expert consensus recommendations of the American society of Neuroradiology. *Am. J. Neuroradiol.* **2018**, *39*, E9–E31. [CrossRef]

61. Naghavi, M.; Libby, P.; Falk, E.; Casscells, S.W.; Litovsky, S.; Rumberger, J.; Badimon, J.J.; Stefanadis, C.; Moreno, P.; Pasterkamp, G.; et al. From Vulnerable Plaque to Vulnerable Patient: A Call for New Definitions and Risk Assessment Strategies: Part II. *Circulation* **2003**, *108*, 1772–1778. [CrossRef] [PubMed]

62. Bos, D.; Arshi, B.; van den Bouwhuijsen, Q.J.A.; Ikram, M.K.; Selwaness, M.; Vernooij, M.W.; Kavousi, M.; van der Lugt, A. Atherosclerotic Carotid Plaque Composition and Incident Stroke and Coronary Events. *J. Am. Coll. Cardiol.* **2021**, *77*, 1426–1435. [CrossRef] [PubMed]

63. Kawasaki, T.; Koga, S.; Koga, N.; Noguchi, T.; Tanaka, H.; Koga, H.; Serikawa, T.; Orita, Y.; Ikeda, S.; Mito, T.; et al. Characterization of Hyperintense Plaque with Noncontrast T1-Weighted Cardiac Magnetic Resonance Coronary Plaque Imaging: Comparison with Multislice Computed Tomography and Intravascular Ultrasound. *J. Am. Coll. Cardiol.* **2009**, *2*, 720–728. [CrossRef] [PubMed]

64. Mitchell, C.C.; Wilbrand, S.M.; Kundu, B.; Steffel, C.N.; Varghese, T.; Meshram, N.H.; Li, G.; Cook, T.D.; Salamat, M.S.; Dempsey, R.J. Transcranial Doppler and Microemboli Detection: Relationships to Symptomatic Status and Histopathology Findings. *Ultrasound Med. Biol.* **2017**, *43*, 1861–1867. [CrossRef]

65. Spence, J.D. Transcranial Doppler monitoring for microemboli: A marker of a high-risk carotid plaque. *Semin. Vasc. Surg.* **2017**, *30*, 62–66. [CrossRef]

66. Spence, J.D.; Tamayo, A.; Lownie, S.P.; Ng, W.P.; Ferguson, G.G. Absence of microemboli on transcranial Doppler identifies low-risk patients with asymptomatic carotid stenosis. *Stroke* **2005**, *36*, 2373–2378. [CrossRef]

67. Markus, H.S.; King, A.; Shipley, M.; Topakian, R.; Cullinane, M.; Reihill, S.; Bornstein, N.M.; Schaafsma, A. Asymptomatic embolisation for prediction of stroke in the Asymptomatic Carotid Emboli Study (ACES): A prospective observational study. *Lancet Neurol.* **2010**, *9*, 663–671. [CrossRef] [PubMed]

68. Eliaszwiw, M.; Rankin, R.N.; Fox, A.J.; Haynes, R.B.; Barnett, H.J. Accuracy and prognostic consequences of ultrasonography in identifying severe carotid artery stenosis. North American Symptomatic Carotid Endarterectomy Trial (NASCET). *Stroke* **1995**, *26*, 1747–1752. [CrossRef]

69. Saba, L.; Caddeo, G.; Sanfilippo, R.; Montisci, R.; Mallarini, G. Efficacy and sensitivity of axial scans and different reconstruction methods in the study of the ulcerated carotid plaque using multidetector-row CT angiography: Comparison with surgical results. *Am. J. Neuroradiol.* **2007**, *28*, 716–723. [CrossRef]

70. Kuk, M.; Wannarong, T.; Beletsky, V.; Parraga, G.; Fenster, A.; Spence, J.D. Volume of carotid artery ulceration as a predictor of cardiovascular events. *Stroke* **2014**, *45*, 1437–1441. [CrossRef]

71. Saba, L.; Tamponi, E.; Raz, E.; Lai, L.; Montisci, R.; Piga, M.; Faa, G. Correlation between fissured fibrous cap and contrast enhancement: Preliminary results with the use of CTA and histologic validation. *Am. J. Neuroradiol.* **2014**, *35*, 754–759. [CrossRef] [PubMed]

72. Romero, J.M.; Babiarz, L.S.; Forero, N.P.; Murphy, E.K.; Schaefer, P.W.; Gonzalez, R.G.; Lev, M.H. Arterial wall enhancement overlying carotid plaque on CT angiography correlates with symptoms in patients with high grade stenosis. *Stroke* **2009**, *40*, 1894–1896. [CrossRef] [PubMed]

73. Arous, E.J.; Judelson, D.R.; Agrawal, A.; Dundamadappa, S.K.; Crawford, A.S.; Malka, K.T.; Simons, J.P.; Schanzer, A. Computed tomography angiography-derived area stenosis calculations overestimate degree of carotid stenosis compared with North American Symptomatic Carotid Endarterectomy Trial-derived diameter stenosis calculations. *J. Vasc. Surg.* **2021**, *74*, 579–585. [CrossRef]

74. Davidhi, A.; Rafailidis, V.; Destanis, E.; Prassopoulos, P.; Foinitsis, S. Ultrasound Elastography: Another piece in the puzzle of carotid plaque vulnerability? *Med. Ultrason.* **2022**, *24*, 356–363. [CrossRef]

75. Meairs, S.; Hennerici, M. Four-dimensional ultrasonographic characterization of plaque surface motion in patients with symptomatic and asymptomatic carotid artery stenosis. *Stroke* **1999**, *30*, 1807–1813. [CrossRef] [PubMed]

76. Muraki, M.; Mikami, T.; Yoshimoto, T.; Fujimoto, S.; Kitaguchi, M.; Kaga, S.; Sugawara, T.; Tokuda, K.; Kaneko, S.; Kashiwaba, T. Sonographic Detection Of Abnormal Plaque Motion Of The Carotid Artery: Its Usefulness In Diagnosing High-Risk Lesions Ranging From Plaque Rupture To Ulcer Formation. *Ultrasound Med. Biol.* **2015**, *42*, 358–364. [CrossRef]

77. Kume, S.; Hama, S.; Yamane, K.; Wada, S.; Nishida, T.; Kurisu, K. Vulnerable carotid arterial plaque causing repeated ischemic stroke can be detected with B-mode ultrasonography as a mobile component: Jellyfish sign. *Neurosurg. Rev.* **2010**, *33*, 419–430. [CrossRef]

78. Johri, A.M.; Herr, J.E.; Li, T.Y.; Yau, O.; Nambi, V. Novel Ultrasound Methods to Investigate Carotid Artery Plaque Vulnerability. *J. Am. Soc. Echocardiogr.* **2017**, *30*, 139–148. [CrossRef]

79. Sluimer, J.C.; Daemen, M.J. Novel concepts in atherogenesis: Angiogenesis and hypoxia in atherosclerosis. *J. Pathol.* **2009**, *218*, 7–29. [CrossRef]

80. Puchner, S.B.; Liu, T.; Mayrhofer, T.; Truong, Q.A.; Lee, H.; Fleg, J.L.; Nagurney, J.T.; Udelson, J.E.; Hoffmann, U.; Ferencik, M. High-risk plaque detected on coronary CT angiography predicts acute coronary syndromes independent of significant stenosis in acute chest pain: Results from the ROMICAT-II trial. *J. Am. Coll. Cardiol.* **2014**, *64*, 684–692. [CrossRef]

81. Newby, D.E.; Adamson, P.D.; Berry, C.; Boon, N.A.; Dweck, M.R.; Flather, M.; Forbes, J.; Hunter, A.; Lewis, S.; MacLean, S.; et al. Coronary CT angiography and 5-Year risk of myocardial infarction. *N. Engl. J. Med.* **2018**, *379*, 924–933. [PubMed]

82. Ambrose, J.A.; Tannenbaum, M.A.; Alexopoulos, D.; Hjemdahl-Monsen, C.E.; Leavy, J.; Weiss, M.; Borrico, S.; Gorlin, R.; Fuster, V. Angiographic progression of coronary artery disease and the development of myocardial infarction. *J. Am. Coll. Cardiol.* **1988**, *12*, 56–62. [CrossRef] [PubMed]

83. Wasserman, B.A.; Wityk, R.J.; Trout, H.H.; Virmani, R. Low-grade carotid stenosis: Looking beyond the lumen with MRI. *Stroke* **2005**, *36*, 2504–2513. [CrossRef] [PubMed]

84. Huang, X.; Yin, X.; Xu, Y.; Jia, X.; Li, J.; Niu, P.; Shen, W.; Kassab, G.S.; Tan, W.; Huo, Y. Morphometric and hemodynamic analysis of atherosclerotic progression in human carotid artery bifurcations. *Am. J. Physiol. Heart Circ. Physiol.* **2016**, *310*, H639–H647. [CrossRef]

85. Johnsen, S.H.; Mathiesen, E.B. Carotid plaque compared with intima-media thickness as a predictor of coronary and cerebrovascular disease. *Curr. Cardiol.* **2009**, *11*, 21–27. [CrossRef]

86. Brinjikji, W.; Huston, J.I.; Rabinstein, A.A.; Kim, G.M.; Lerman, A.; Lanzino, G. Contemporary carotid imaging: From degree of stenosis to plaque vulnerability. *J. Neurosurg.* **2016**, *124*, 27–42. [CrossRef]

87. Tagliafico, A.S.; Piana, M.; Schenone, D.; Lai, R.; Massone, A.M.; Houssami, N. Overview of radiomics in breast cancer diagnosis and prognostication. *Breast* **2020**, *49*, 74–80. [CrossRef]

88. Zhou, R.; Ma, W.; Fenster, A.; Ding, M. U-Net based automatic carotid plaque segmentation from 3D ultrasound images. In Proceedings of the Medical Imaging 2019: Computer-Aided Diagnosis, San Diego, CA, USA, 16–21 February 2019; Volume 0950, pp. 1119–1125.

89. Available online: https://www.kaggle.com/c/carvana-image-masking-challenge (accessed on 27 February 2023).

90. Available online: https://github.com/lyakaap/Kaggle-Carvana-3rd-Place-Solution (accessed on 27 February 2023).

91. Meshram, N.H.; Mitchell, C.C.; Wilbrand, S.M. Deep learning for carotid plaque segmentation using a dilated UNet architecture. *Ultrason. Imaging* **2020**, *42*, 221–230. [CrossRef]

92. Loizou, C.P.; Pattichis, C.S.; Pantziaris, M.; Tyllis, T.; Nicolaides, A. Snakes based segmentation of the common carotid artery intima media. *Med. Biol. Eng. Comput.* **2007**, *45*, 35–49. [CrossRef]

93. Menchón-Lara, R.M.; Sancho-Gómez, J.L. Fully automatic segmentation of ultrasound common carotid artery images based on machine learning. *Neurocomputing* **2015**, *151*, 161–167. [CrossRef]

94. Biswas, M.; Kuppili, V.; Araki, T.; Edla, D.R.; Godia, E.C.; Saba, L.; Suri, H.S.; Omerzu, T.; Laird, J.R.; Khanna, N.N.; et al. Deep learning strategy for accurate carotid intima-media thickness measurement: An ultrasound study on Japanese diabetic cohort. *Comput. Biol. Med.* **2018**, *98*, 100–117. [CrossRef] [PubMed]

95. Qiu, Z.; Langerman, J.; Nair, N.; Aristizabal, O.; Mamou, J.; Turnbull, D.H.; Ketterling, J.; Wang, Y. DEEP BV: A Fully Automated System for Brain Ventricle Localization and Segmentation in 3D Ultrasound Images of Embryonic Mice. In Proceedings of the IEEE Signal Processing in Medicine and Biology Symposium (SPMB), Philadelphia, PA, USA, 1 December 2018; pp. 1–6.

96. Amiri, M.; Brooks, R.; Behboodi, B.; Rivaz, H. Two-stage ultrasound image segmentation using U-Net and test time augmentation. *Int. J. Comput. Assist. Radiol. Surg.* **2020**, *15*, 981–988. [CrossRef] [PubMed]

97. Jain, P.K.; Sharma, N.; Saba, L.; Paraskevas, K.I.; Kalra, M.K.; Johri, A.; Laird, J.R.; Nicolaides, A.N.; Suri, J.S. Unseen Artificial Intelligence—Deep Learning Paradigm for Segmentation of Low Atherosclerotic Plaque in Carotid Ultrasound: A Multicenter Cardiovascular Study. *Diagnostics* **2021**, *11*, 2257. [CrossRef] [PubMed]

98. Zhang, L.; Lyu, Q.; Ding, Y.; Hu, C.; Hui, P. Texture Analysis Based on Vascular Ultrasound to Identify the Vulnerable Carotid Plaques. *Front. Neurosci.* **2022**, *16*, 885209. [CrossRef] [PubMed]

99. Skandha, S.S.; Gupta, S.K.; Saba, L.; Koppula, V.K.; Johri, A.M.; Khanna, N.N.; Mavrogeni, S.; Laird, J.R.; Pareek, G.; Miner, M.; et al. 3-D optimized classification and characterization artificial intelligence paradigm for cardiovascular/stroke risk stratification using carotid ultrasound-based delineated plaque: Atheromatic™ 2.0. *Comput. Biol. Med.* **2020**, *125*, 103958. [CrossRef] [PubMed]

100. Sousa, L.C.; Castro, C.F.; Antonio, C.C.; Sousa, F.; Santos, R.; Castro, P.; Azevedo, E. Computational simulation of carotid stenosis and flow dynamics based 4 on patient ultrasound data—A new tool for risk assessment and 5 surgical planning. *Adv. Med. Sci.* **2016**, *61*, 32–39. [CrossRef]

101. Coli, S.; Magnoni, M.; Sangiorgi, G.; Marrocco-Trischitta, M.M.; Melisurgo, G.; Mauriello, A.; Spagnoli, L.; Chiesa, R.; Cianflone, D.; Maseri, A. Contrast-Enhanced ultrasound imaging of intraplaque neovascularization in carotid arteries correlation with histology and plaque echogenicity. *J. Am. Coll. Cardiol.* **2008**, *52*, 223–230. [CrossRef]

102. Staub, D.; Patel, M.B.; Tibrewala, A.; Ludden, D.; Johnson, M.; Espinosa, P.; Coll, B.; Jaeger, K.A.; Feinstein, S.B. Vasa vasorum and plaque neovascularization on contrast-enhanced carotid ultrasound imaging correlates with cardiovascular disease and past cardiovascular events. *Stroke* **2010**, *41*, 41–47. [CrossRef]

103. Akkus, Z.; van Burken, G.; van den Oord, S.; Schinkel, A.F.L.; de Jong, N.; van der Steen, A.F.W.; Bosch, J.G. Carotid intraplaque neovascularization quantification software (CINQS). *IEEE J. Biomed. Health Inform.* **2015**, *19*, 332–338. [CrossRef]

104. Svedlund, S.; Gan, L.M. Longitudinal common carotid artery wall motion is associated with plaque burden in man and mouse. *Atherosclerosis* **2011**, *217*, 120–124. [CrossRef]

105. Ogata, T.; Yasaka, M.; Wakugawa, Y.; Kitazono, T.; Okada, Y. Morphological classification of mobile plaques and their association with early recurrence of stroke. *Cerebrovasc. Dis.* **2010**, *30*, 606–611. [CrossRef] [PubMed]

106. Dempsey, R.J.; Varghese, T.; Jackson, D.C.; Wang, X.; Meshram, N.H.; Mitchell, C.C.; Hermann, B.P.; Johnson, S.C.; Berman, S.E.; Wilbrand, S.M. Carotid atherosclerotic plaque instability and cognition determined by ultrasound-measured plaque strain in asymptomatic patients with significant stenosis. *J. Neurosurg.* **2018**, *128*, 111–119. [CrossRef] [PubMed]

107. Steinbuch, J.; Hoeks, A.P.G.; Hermeling, E.; Truijman, M.T.B.; Schreuder, F.H.B.M.; Mess, W.H. Standard b-mode ultrasound measures local carotid artery characteristics as reliably as radiofrequency phase tracking in symptomatic carotid artery patients. *Ultrasound Med. Biol.* **2016**, *42*, 586–595. [CrossRef] [PubMed]

108. Azzopardi, C.; Camilleri, K.P.; Hicks, Y.A. Bimodal Automated Carotid Ultrasound Segmentation using Geometrically Constrained Convolutional Neural Networks. *J. Biomed. Health Inform.* **2019**, *24*, 1004–1015. [CrossRef] [PubMed]

109. Saba, B.; Mainak, O.; Tomaž, L.; Johri, A.M.; Khanna, N.N.; Viskovic, K.; Mavrogeni, S.; Laird, J.R.; Pareek, G.; Miner, M.; et al. A Review on Joint Carotid Intima-Media Thickness and Plaque Area Measurement in Ultrasound for Cardiovascular/Stroke Risk Monitoring: Artificial Intelligence Framework. *J. Digit. Imaging* **2021**, *34*, 581–604.

110. Jamthikar, A.; Gupta, D.; Saba, L.; Khanna, N.N.; Viskovic, K.; Mavrogeni, S.; Laird, J.R.; Sattar, N.; Johri, A.M.; Pareek, G.; et al. Artificial Intelligence Framework for Predictive Cardiovascular and Stroke Risk Assessment Models: A Narrative Review of Integrated Approaches using Carotid Ultrasound. *Comput. Biol. Med.* **2020**, *126*, 104043. [CrossRef]

111. Johri, A.M.; Mantella, L.E.; Jamthikar, A.D.; Saba, L.; Laird, J.R.; Suri, J.S. Role of artifcial intelligence in cardiovascular risk prediction and outcomes: Comparison of machine-learning and conventional statistical approaches for the analysis of carotid ultrasound features and intra-plaque neovascularization. *Int. J. Cardiovasc. Imaging* **2021**, *37*, 3145–3156. [CrossRef]

112. Csippa, B.; Mihály, Z.; Czinege, Z.; Németh, M.B.; Halász, G.; Paál, G.; Sótonyi, P., Jr. Comparison of Manual versus Semi-Automatic Segmentations of the Stenotic Carotid Artery Bifurcation. *Appl. Sci.* **2021**, *11*, 8192. [CrossRef]

113. Scherl, H.; Hornegger, J.; Prümmer, M.; Lell, M. Semi-automatic level-set based segmentation and stenosis quantification of the internal carotid artery in 3D CTA data sets. *Med. Image Anal.* **2007**, *11*, 21–34. [CrossRef]

114. Cau, R.; Flanders, A.; Mannelli, L.; Politi, C.; Faa, G.; Suri, J.S.; Saba, L. Artificial intelligence in computed tomography plaque characterization: A review. *Eur. J. Radiol.* **2021**, *140*, 109767. [CrossRef]

115. Klimont, M.; Oronowicz-Jaśkowiak, A.; Flieger, M.; Rzeszutek, J.; Juszkat, R.; Jończyk-Potoczna, K. Deep learning for cerebral angiography segmentation from non-contrast computed tomography. *PLoS ONE* **2020**, *15*, e0237092. [CrossRef] [PubMed]

116. Richardson, M.L.; Garwood, E.R.; Lee, Y.; Li, M.D.; Lo, H.S.; Nagaraju, A.; Nguyen, X.V.; Probyn, L.; Rajiah, P.; Sin, J.; et al. Non interpretive uses of artificial intelligence in radiology. *Acad. Radiol.* **2020**, *28*, 1225–1235. [CrossRef] [PubMed]

117. Van Assen, M.; Muscogiuri, G.; Caruso, D.; Lee, S.J.; Laghi, A.; De Cecco, C.N. Artificial intelligence in cardiac radiology. *Radiol. Med.* **2020**, *125*, 1186–1199. [CrossRef] [PubMed]

118. Eberhard, M.; Alkadhi, H. Machine learning and deep neural networks: Applications in patient and scan preparation, contrast medium, and radiation dose optimization. *J. Thorac. Imaging* **2020**, *35*, 17–20. [CrossRef]

119. Korporaal, J.G.; Mahnken, A.H.; Ferda, J.; Hausleiter, J.; Baxa, J.; Hadamitzky, M.; Flohr, T.G.; Schmidt, B.T. Quantitative evaluation of the performance of a new test bolus–Based computed tomographic angiography contrast-enhancement–Prediction algorithm. *Investig. Radiol.* **2015**, *50*, 1–8. [CrossRef]

120. Xie, S.; Zheng, X.; Chen, Y.; Xie, L.; Liu, J.; Zhang, Y.; Yan, J.; Zhu, H.; Hu, Y. Artifact removal using improved GoogLeNet for sparse-view CT reconstruction. *Sci. Rep.* **2018**, *8*, 6700. [CrossRef]

121. Gudigar, A.; Nayak, S.; Samanth, J.; Raghavendra, U.; Ashwal, A.J.; Barua, P.D.; Hasan, M.N.; Ciaccio, E.J.; Tan, R.; Acharya, U.R. Recent Trends in Artificial Intelligence-Assisted Coronary Atherosclerotic Plaque Characterization. *Int. J. Environ. Res. Public Health* **2021**, *18*, 10003. [CrossRef]

122. Buckler, A.J.; Gotto AMJr Rajeev, A.; Nicolaou, A.; Sakamoto, A.; St Pierre, S.; Phillips, M.; Virmani, R.; Villines, T.C. Atherosclerosis risk classification with computed tomography angiography: A radiologic-pathologic validation study. *Atherosclerosis* **2023**, *366*, 42–48. [CrossRef]

123. Kamtchum-Tatuene, J.; Wilman, A.; Saqqur, M.; Shuaib, A.; Jickling, G.C. Carotid plaque with high-risk features in embolic stroke of undetermined source: Systematic review and meta-analysis. *Stroke* **2020**, *51*, 311–314. [CrossRef]

124. Le, E.P.V.; Rundo, L.; Tarkin, J.; Evans, N.R.; Chowdhury, M.M.; Coughlin, P.A.; Pavey, H.; Wall, C.; Zaccagna, F.; Gallagher, F.A.; et al. Assessing robustness of carotid artery CT angiography radiomics in the identification of culprit lesions in cerebrovascular events. *Sci. Rep.* **2021**, *11*, 3499. [CrossRef]

125. Kigka, V.I.; Sakellarios, A.I.; Mantzaris, M.D.; Tsakanikas, V.D.; Potsika, V.T.; Palombo, D.; Montecucco, F.; Fotiadis, D.I. A Machine Learning Model for the Identification of High risk Carotid Atherosclerotic Plaques. In Proceedings of the 2021 43rd Annual International Conference of the IEEE Engineering in Medicine & Biology Society (EMBC), Virtual, 1–5 November 2021; pp. 2266–2269.

126. Kigka, V.I.; Sakellarios, A.I.; Tsakanikas, V.D.; Potsika, V.T.; Koncar, I.; Fotiadis, D.I. Detection of Asymptomatic Carotid Artery Stenosis through Machine Learning. In Proceedings of the 2022 44th Annual International Conference of the IEEE Engineering in Medicine & Biology Society (EMBC), Glasgow, UK, 11–15 July 2022; pp. 1041–1044.

127. Rava, R.A.; Peterson, B.A.; Seymour, S.E.; Snyder, K.V.; Mokin, M.; Waqas, M.; Hoi, Y.; Davies, J.M.; Levy, E.I.; Siddiqui, A.H.; et al. Validation of an artificial intelligence-driven large vessel occlusion detection algorithm for acute ischemic stroke patients. *Neuroradiol. J.* **2021**, *34*, 408–417. [CrossRef] [PubMed]

128. Rodrigues, G.; Barreira, C.M.; Bouslama, M.; Snyder, K.V.; Mokin, M.; Waqas, M.; Hoi, Y.; Davies, J.M.; Levy, E.I.; Siddiqui, A.H.; et al. Automated Large Artery Occlusion Detection in Stroke: A Single-Center Validation Study of an Artificial Intelligence Algorithm. *Cerebrovasc. Dis.* **2022**, *51*, 259–264. [CrossRef] [PubMed]

129. Tatsugami, F.; Higaki, T.; Nakamura, Y.; Yu, Z.; Zhou, J.; Lu, Y.; Fujioka, C.; Kitagawa, T.; Kihara, Y.; Iida, M.; et al. Deep learning–based image restoration algorithm for coronary CT angiography. *Eur. Radiol.* **2019**, *29*, 5322–5329. [CrossRef] [PubMed]

130. Benz, D.C.; Benetos, G.; Rampidis, G.; von Felten, E.; Bakula, A.; Sustar, A.; Kudura, K.; Messerli, M.; Fuchs, T.A.; Gebhard, C.; et al. Validation of deep-learning image reconstruction for coronary computed tomography angiography: Impact on noise, image quality and diagnostic accuracy. *J. Cardiovasc. Comput. Tomogr.* **2020**, *14*, 444–451. [CrossRef]

131. Ajami, M.; Tripathi, P.; Ling, H.; Mahdian, M. Automated Detection of Cervical Carotid Artery Calcifications in Cone Beam Computed Tomographic Images Using Deep Convolutional Neural Networks. *Diagnostics* **2022**, *12*, 2537. [CrossRef] [PubMed]

132. Chandrashekar, A.; Handa, A.; Shivakumar, N.; Lapolla, P.; Uberoi, R.; Grau, V.; Lee, R. A Deep Learning Pipeline to Automate High-Resolution Arterial Segmentation With or Without Intravenous Contrast. *Ann. Surg.* **2022**, *276*, e1017–e1027. [CrossRef]

133. Olive-Gadea, M.; Crespo, C.; Granes, C.; Hernandez-Perez, M.; Pérez de la Ossa, N.; Laredo, C.; Urra, X.; Soler, J.C.; Soler, A.; Puyalto, P.; et al. Deep Learning Based Software to Identify Large Vessel Occlusion on Noncontrast Computed Tomography. *Stroke* **2020**, *51*, 3133–3137. [CrossRef]

134. Ingersleben, G.V.; Schmiedl, U.P.; Hatsukami, T.S.; Nelson, J.A.; Subramaniam, D.S.; Ferguson, M.S.; Yuan, C. Characterization of atherosclerotic plaques at the carotid bifurcation: Correlation of high resolution MR with histology. *Radiographic* **1997**, *17*, 1417–1423. [CrossRef]

135. Toussaint, J.F.; LaMuraglia, G.M.; Southern, J.R.; Fuster, V.; Kantor, H.L. Magnetic resonance images lipid, fibrous, calcified, hemorrhagic, and thrombotic components of human atherosclerosis in vivo. *Circulation* **1996**, *94*, 932–938. [CrossRef]

136. Martin, A.J.; Gotlieb, A.I.; Henkelman, R.M. High resolution MR imaging of human arteries. *JMRI* **1995**, *5*, 93–100. [CrossRef]

137. Merickel, M.B.; Berr, S.; Spetz, K.; Jackson, T.R.; Snell, J.; Gillies, P.; Shimshick, E.; Hainer, J.; Brookeman, J.R.; Ayers, C.R. Non-invasive quantitative evaluation of atherosclerosis using MRI and image analysis. *Arterioscler. Thromb.* **1993**, *13*, 1180–1186. [CrossRef] [PubMed]

138. Kang, X.; Polissar, N.L.; Han, C.; Lin, E.; Yuan, C. Analysis of the measurement precision of arterial lumen and wall areas using high-resolution MRI. *Magn. Reason. Med.* **2000**, *44*, 968–972. [CrossRef]

139. Zhao, X.; Li, R.; Hippe, D.S.; Hatsukami, T.S.; Yuan, C. Chinese Atherosclerosis Risk Evaluation (CARE II) study: A novel cross-sectional, multicentre study of the prevalence of high-risk atherosclerotic carotid plaque in Chinese patients with ischaemic cerebrovascular events-design and rationale. *Stroke Vasc. Neurol.* **2017**, *2*, 15–20. [CrossRef] [PubMed]

140. Saam, T.; Hatsukami, T.S.; Takaya, N.; Chu, B.; Underhill, H.; Kerwin, W.S.; Cai, J.; Ferguson, M.S.; Yuan, C. The vulnerable, or high-risk, atherosclerotic plaque: Noninvasive MR imaging for characterization and assessment. *Radiology* **2007**, *244*, 64–77. [CrossRef] [PubMed]

141. Moody, A.R.; Murphy, R.E.; Morgan, P.S.; Martel, A.L.; Delay, G.S.; Allder, S.; MacSweeney, S.T.; Tennant, W.G.; Gladman, J.; Lowe, J.; et al. Characterization of complicated carotid plaque with magnetic resonance direct thrombus imaging in patients with cerebral ischemia. *Circulation* **2003**, *108*, 847–853. [CrossRef] [PubMed]

142. Takaya, N.; Yuan, C.; Chu, B.; Saam, T.; Underhill, H.; Cai, J.; Tran, N.; Polissar, N.L.; Isaac, C.; Ferguson, M.S.; et al. Association Between Carotid Plaque Characteristics and Subsequent Ischemic Cerebrovascular Events. *Stroke.* **2006**, *37*, 818–823. [CrossRef]

143. Murphy, R.E.; Moody, A.R.; Morgan, P.S.; Martel, A.L.; Delay, G.S.; Allder, S.; MacSweeney, S.T.; Tennant, W.G.; Gladman, J.; Lowe, J.; et al. Prevalence of complicated carotid atheroma as detected by magnetic resonance direct thrombus imaging in patients with suspected carotid artery stenosis and previous acute cerebral ischemia. *Circulation* **2003**, *107*, 3053–3058. [CrossRef]

144. Zhao, X.; Hippe, D.S.; Li, R.; Sui, B.; Song, Y.; Li, F.; Xue, Y.; Sun, J.; Yamada, K.; Hatsukami, T.S.; et al. Prevalence and characteristics of carotid artery high -risk atherosclerotic plaques in Chinese patients with cerebrovascular symptoms: A Chinese atherosclerosis risk evaluation II study. *J. Am. Heart Assoc.* **2017**, *6*, e005831. [CrossRef]

145. Freilinger, T.M.; Schindler, A.; Schmidt, C.; Grimm, J.; Cyran, C.; Schwarz, F.; Bamberg, F.; Linn, J.; Reiser, M.; Yuan, C.; et al. Prevalence of nonstenosing, complicated atherosclerotic plaques in cryptogenic stroke. *JACC Cardiovasc. Imaging* **2012**, *5*, 397–405. [CrossRef]

146. Mandell, D.M.; Mossa-Basha, M.; Qiao, Y.; Hess, C.P.; Hui, F.; Matouk, C.; Johnson, M.H.; Daemen, M.J.A.P.; Vossough, A.; Edjlali, M.; et al. Intracranial vessel wall MRI: Principles and expert consensus recommendations of the American Society of Neuroradiology. *Am. J. Neuroradiol.* **2017**, *38*, 218–229. [CrossRef]

147. Tian, Y.; Chen, Q.; Wang, W.; Peng, Y.; Wang, Q.; Duan, F.; Wu, Z.; Zhou, M. A vessel active contour model for vascular segmentation. *BioMed Res. Int.* **2014**, *2014*, 106490. [CrossRef]

148. Yuan, C.; Lin, E.; Millard, J.; Hwang, J.N. Closed contour edge detection of blood vessel lumen and outer wall boundaries in black-blood MR images. *Magn. Reason. Imaging* **1999**, *17*, 257–266. [CrossRef] [PubMed]

149. Adams, G.J.; Vick, I.I.I.G.W.; Bordelon, C.B.; Insull, W.; Morrisett, J. Algorithm for quantifying advanced carotid artery atherosclerosis in humans using MRI and active contours. *Proc. SPIE* **2002**, *4684*, 1448–1457.

150. Alblas, D.; Brune, C.; Wolterink, J.M. Deep-Learning-Based Carotid Artery Vessel Wall Segmentation in Black-Blood MRI Using Anatomical Priors. In Proceedings of the SPIE Medical Imaging 2022: Image Processing, San Diego, CA, USA, 20 February–28 March 2022; Volume 12032, pp. 1605–7422.

151. Yuan, C.; Chen, L.; Balu, N.; Mossa-Basha, M.; Hwang, J.N. Carotid Artery Vessel Wall Segmentation Challenge. 2021. Available online: https://vessel-wall-segmentation.grand-challenge.org (accessed on 27 February 2023).

152. Adame, I.M.; van der Geest, R.J.; Wasserman, B.A.; Mohamed, M.A.; Reiber, J.H.C.; Lelieveldt, B.F.P. Automatic segmentation and plaque characterization in atherosclerotic carotid artery MR images. *MAGMA* **2004**, *16*, 227–234. [CrossRef]

153. Yang, F.; Holzapfel, G.; Schulze-Bauer, C.; Stollberger, R.; Thedens, D.; Bolinger, L.; Stolpen, A.; Sonka, M. Segmentation of wall and plaque in in vitro vascular MR images. *Int. J. Cardiovasc. Imaging* **2003**, *19*, 419–428. [CrossRef]

154. Wu, J.; Xin, J.; Yang, X.; Sun, J.; Xu, D.; Zheng, N.; Yuan, C. Deep morphology aided diagnosis network for segmentation of carotid artery vessel wall and diagnosis of carotid atherosclerosis on black-blood vessel wall MRI. *Med. Phys.* **2019**, *46*, 5544–5561. [CrossRef]

155. Tsakanikas, V.D.; Siogkas, P.K.; Mantzaris, M.D.; Potsika, V.T.; Kigka, V.I.; Exarchos, T.P.; Koncar, I.B.; Jovanović, M.; Vujčić, A.; Dučić, S.; et al. A deep learning oriented method for automated 3D reconstruction of carotid arterial trees from MR imaging. In Proceedings of the 2020 42nd Annual International Conference of the IEEE Engineering in Medicine and Biology Society (EMBC), Montreal, QC, Canada, 20–24 July 2020; pp. 2408–2411.

156. Timmerman, N.; Galyfos, G.; Sigala, F.; Sun, J.; Xu, D.; Zheng, N.; Yuan, C. The TAXINOMISIS Project: A multidisciplinary approach for the development of a new risk stratification model for patients with asymptomatic carotid artery stenosis. *Eur. J. Clin Investig.* **2020**, *50*, e13411. [CrossRef]

157. Shi, Z.; Zhu, C.; Degnan, A.J.; Tian, X.; Li, J.; Chen, L.; Zhang, X.; Peng, W.; Chen, C.; Lu, J.; et al. Identification of high-risk plaque features in intracranial atherosclerosis: Initial experience using a radiomic approach. *Eur. Radiol.* **2018**, *28*, 3912–3921. [CrossRef]

158. Shi, Z.; Li, J.; Zhao, M.; Peng, W.; Meddings, Z.; Jiang, T.; Liu, Q.; Teng, Z.; Lu, J. Quantitative histogram analysis on intracranial atherosclerotic plaques: A high-resolution magnetic resonance imaging study. *Stroke* **2020**, *51*, 2161–2169. [CrossRef]

159. Zhang, R.; Zhang, Q.; Ji, A.; Lv, P.; Zhang, J.; Fu, C.; Lin, J. Identification of high-risk carotid plaque with MRI-based radiomics and machine learning. *Eur. Soc. Radiol.* **2021**, *31*, 3116–3126. [CrossRef]

160. Lindner, J.R. Microbubbles in medical imaging: Current applications and future directions. *Nat. Rev. Drug Discov.* **2004**, *3*, 527–532. [CrossRef]

161. Lindner, J.R.; Dayton, P.A.; Coggins, M.P.; Ley, K.; Song, J.; Ferrara, K.; Kaul, S. Noninvasive imaging of inflammation by ultrasound detection of phagocytosed microbubbles. *Circulation* **2000**, *102*, 531–538. [CrossRef] [PubMed]

162. Owen, D.R.; Shalhoub, J.; Miller, S.; Gauthier, T.; Doryforou, O.; Davies, A.H.; Leen, E.L.S. Inflammation within carotid atherosclerotic plaque: Assessment with late-phase contrast-enhanced US. *Radiology* **2010**, *255*, 638–644. [CrossRef]

163. Shalhoub, J.; Monaco, C.; Owen, D.R.; Gauthier, T.; Thapar, A.; Leen, E.L.S.; Davies, A.H. Late-phase contrast-enhanced ultrasound reflects biological features of instability in human carotid atherosclerosis. *Stroke* **2011**, *42*, 3634–3636. [CrossRef]

164. Lerman, L.O.; Rodriguez-Porcel, M.; Krier, J.D.; Moody, J.; Moffat, B.F.; Hall, D.E.; Kim, G.; Koo, Y.E.L.; Woolliscroft, M.J.; Sugai, J.V.; et al. Vascular targeted nanoparticles for imaging and treatment of atherosclerosis. *JACC Cardiovasc. Imaging* **2009**, *2*, 350–360.

165. Li, X.; Wu, M.; Li, J.; Guo, Q.; Zhao, Y.; Zhang, X. Advanced targeted nanomedicines for vulnerable atherosclerosis plaque imaging and their potential clinical implications. *Front. Pharmacol.* **2022**, *13*, 906512. [CrossRef]

166. Guo, B.; Li, Z.; Tu, P.; Tang, H.; Tu, Y. Molecular imaging and non−molecular imaging of atherosclerotic plaque thrombosis. *Front. Cardiovasc. Med.* **2021**, *8*, 692915. [CrossRef]

167. González-García, H.; Díaz-Sánchez, S.; Herraiz-Martínez, A.; Liu, R.; Han, Y.; Li, M.; Wang, F.; Yang, Q.; Zhu, W.; Ye, R.; et al. Optical coherence tomography in carotid artery disease: A systematic review. *Neurologia* **2021**, *36*, 16–27.

168. Yang, Q.; Guo, H.; Shi, X.; Xu, X.; Zha, M.; Cai, H.; Yang, D.; Huang, F.; Zhang, X.; Lv, Q.; et al. Identification of Symptomatic Carotid Artery Plaque: A Three-Item Scale Combined Angiography With Optical Coherence Tomography. *Front. Neurosci.* **2021**, *15*, 792437. [CrossRef]

169. Piri, R.; Hamakan, Y.; Vang, A.; Edenbrandt, L.; Larsson, M.; Enqvist, O.; Gerke, O.; Høilund-Carlsen, P.F. Common carotid segmentation in ^{18}F-sodium fluoride PET/CT scans: Head-to-head comparison of artificial intelligence-based and manual method. *Clin. Physiol. Funct. Imaging* **2023**, *43*, 71–77. [CrossRef]